Sambaya et al. *Zool. Res. Divers. Conserv.* 2025, 2(4): 233−249
https://doi.org/10.24272/j.issn.2097-3772.2025.030
https://cstr.cn/32249.14.zrdc.2025.030

ZRDC Zoological Research: Diversity and Conservation

Article Open Access

Integrative phylogeography of African striped grass mice *(Lemniscomys)*: Cryptic diversity and habitat resilience

Brian Anoto Sambaya[1,2,3,#], Samson Mabeya Ouru[1,2,3,#], Shui-Wang He[1], Simon Musila[3], Quan Li[1], Zhong-Zheng Chen[1,4], Wen-Yu Song[1,5], Xue-You Li[1], Kenneth Otieno Onditi[1,3,6,*], Xue-Long Jiang[1,6,*]

[1] *State Key Laboratory of Genetic Evolution and Animal Models*, *Kunming Institute of Zoology*, *Chinese Academy of Sciences*, *Kunming*, *Yunnan* 650201, *China*

[2] *Kunming College of Life Sciences*, *University of Chinese Academy of Sciences*, *Kunming*, *Yunnan* 650201, *China*

[3] *Mammal Section*, *Department of Zoology*, *National Museums of Kenya*, *Nairobi* 40658-00100, *Kenya*

[4] *Collaborative Innovation Centre of Recovery and Reconstruction of Degraded Ecosystem in Wanjiang Basin Co-founded by Anhui Province and Ministry of Education*, *School of Ecology and Environment*, *Anhui Normal University*, *Wuhu*, *Anhui* 241002, *China*

[5] *Vector Laboratory*, *Institute of Pathogens and Vectors*, *Yunnan Provincial Key Laboratory for Zoonosis Control and Prevention*, *Dali University*, *Dali*, *Yunnan* 671003, *China*

[6] *Sino-Africa Joint Research Centre*, *Chinese Academy of Sciences*, *Nairobi* 62000-00200, *Kenya*

ABSTRACT

Small mammals serve as important model organisms for studying how climate and human activities influence biodiversity and human–animal interactions. However, their ecological and phylogeographic histories, and how these relate to rapid climate and land-use changes, remain poorly understood. The pan-African open-habitat murine genus *Lemniscomys* (striped grass mice) illustrates this pattern. Using the most comprehensive genetic data for this genus, we combined integrative phylogenetics, divergence dating, and ancestral-range reconstruction to connect lineage history with spatiotemporal habitat dynamics. We identified 15 molecular operational taxonomic units (MOTUs) corresponding to nine named species, along with cryptic diversity in three species. The genus diverged from its sister lineage (genus *Arvicanthis*) about 2.8 million years ago in the Sudanian Savanna belt, with internal diversification peaking during the early to mid-Pleistocene. Despite ongoing habitat contraction, *Lemniscomys* MOTUs maintained suitable habitats across past and future climate scenarios (from the late Pliocene to the end of the 21st century). Our results clarify the phylogeography of the genus and emphasize the need for a formal reassessment of several traditional lineages to reevaluate MOTUs-morphospecies relationships across different sampling depths.

Keywords: *Lemniscomys*; Taxonomy; Evolutionary history; Ancestral range reconstruction; Species distribution modeling; Land-use/land-cover change

INTRODUCTION

Small mammals such as rodents are central to testing how climate dynamics and human land use reshape biodiversity and animal–human interactions (Friant et al., 2025; García-Peña et al., 2021). However, many of these small mammals remain poorly documented with respect to their eco-phylogeographic histories and how those histories intersect with rapid climatic variability and land-use change. The African striped grass mouse (*Lemniscomys* Trouessart, 1881), a lineage of open-habitat murines ranging across continental Africa, is a notable example (Happold, 2013; Wilson et al., 2017).

Contemporary taxonomy recognizes 11 *Lemniscomys* species (Happold, 2013; The American Society of Mammalogist's Mammal Diversity Database, 2025; Wilson et al., 2017). However, the taxonomic classification of the genus remains unsettled (Supplementary Figure S1). Recent genetic investigations show that the current species arrangement does not align with genetic evolutionary lineages, and cryptic genetic structure remains to be reconciled with morphology (Hánová et al., 2021). Moreover, several questions remain regarding the ecological and evolutionary history of *Lemniscomys*, including its broad geographic distribution across forests, savannas, and ecotones; its

Received: 10 October 2025; Accepted: 12 December 2025; Online: 23 December 2025

Foundation items: This research was funded by the Sino-Africa Joint Research Centre, Chinese Academy of Sciences (grant number: SAJC202402).

[#]Authors contributed equally to this work

*Corresponding authors, E-mail: jiangxl@mail.kiz.ac.cn; kenneth@mail.kiz.ac.cn

predominantly diurnal activity patterns; and its apparent tolerance of heterogeneous, disturbance-prone landscapes despite largely avoiding hyper-arid cores and dense rainforest interiors (Happold, 2013; Nicolas et al., 2008). These traits make *Lemniscomys* an ideal model for investigating how shifting climatic regimes and human land conversion in Africa shape population connectivity, spatialtemporal habitat dynamics, and sensitivity to land-use change.

Lemniscomys belongs to the Arvicanthini tribe, which underwent one of Africa's most successful late Miocene radiations (Denys et al., 2017; Mikula et al., 2021). Its colonization of Africa from Asia, followed by rapid diversification, coincided with Messinian climatic drying and the fragmentation of pan-African forests (Ducroz et al., 2001; Mikula et al., 2021). These historical environmental shifts likely opened habitat corridors for grassland-adapted murines while isolating forest specialists and perhaps set the stage for the generalist tendencies observed in *Lemniscomys* (deMenocal, 2004; Lecompte et al., 2008; Mikula et al., 2021). Refined phylogeographic studies within the genus would provide key insights into the connections between Africa's mammalian divergence–dispersal timings, climate oscillations, and biome reorganizations (Couvreur et al., 2021; deMenocal, 2004; Malhi et al., 2013; Neumann & Bamford, 2015). Such a phylogeographic investigation must also account for the interaction between land-use change and climate dynamics as drivers of habitat suitability and fragmentation for these species (Hu et al., 2025; Leirs et al., 2023; Mweu et al., 2024; Olorunfemi et al., 2022; Serneels et al., 2007; Starik et al., 2020).

As potential reservoirs of zoonotic pathogens (Halliday et al., 2015), *Lemniscomys* also straddle the biodiversity–public health interface, where a reliable understanding of their phylogeographic and ecological structures is essential for assessing, mapping, and managing zoonotic risks (Han et al., 2016). Reconstructing their ancestral ranges and modeling species distribution across paleoclimate, current climate, and land-use layers would offer a solid framework to examine whether *Lemniscomys'* apparent ecological generalism indicates repeated range shifts to follow grassland changes, persistence in refugial ecotones, or both, and to predict their sensitivity under likely future scenarios (Guillory & Brown, 2021).

To update the phylogenetic understanding of *Lemniscomys*, explore its biogeographic history, and test ecological–evolutionary hypotheses, we compiled the most comprehensive genetic and morphological dataset available for the genus, including museum samples and new field surveys from Kenya. We (i) reconstructed time-calibrated phylogenies using multilocus datasets to assess the rate of diversification, (ii) analyzed ancestral areas to determine whether divergences align with biome boundaries or geomorphologically mediated corridors, and (iii) applied species distribution models to measure shifts in habitat suitability over space and time. These analyses aim to provide an updated integration of phylogenetic, evolutionary, and population-structuring insights, along with assessments of vulnerability to climatic and human-induced changes within and among *Lemniscomys* species.

MATERIALS AND METHODS

Study area and sampling

We obtained 631 geolocated genotyped samples from the known distribution range of the genus *Lemniscomys* (Supplementary Table S1; Supplementary Figure S2). These samples include 95 sourced from new field surveys conducted in Kenya between 2015 and 2019 (Figure 1D) and 536 from previous studies with publicly available genetic material (Figure 1A-C). The combined dataset included collections from 219 localities across 27 countries, covering all major biogeographic regions where the genus has been recorded.

The new Kenyan field surveys covered a broad ecoclimatic (elevational and habitat) gradient, including the Chyulu Hills (grassland and woodland), Shimba Hills National Reserve (grassland and coastal forest), Loita Hills regions (forest, woodlands, and grasslands), the satellite Mau Forest Complex forests, marsh vegetation, and adjacent farmland in the Yala Swamp, the forests and ecotones of Kakamega Forest, and the windward and leeward slopes of Mount Kenya. These new surveys conducted in Kenya aimed to address gaps in existing collections by focusing on regions and habitats that were previously undersampled. This nationwide coverage captured the main ecoclimatic gradients of the species of interest; however, some areas, particularly the northwest diagonal of the country, are still less well represented, and we hope that future surveys will help fill these gaps. The animal handling procedures in these new field surveys adhered to Kenya's wildlife research regulations and the established guidelines for the use of wild animals in academic research (Sikes & The Animal Care and Use Committee of the American Society of Mammalogists, 2016; Underwood & Anthony, 2020). The research was approved by the Kenya Wildlife Service Research and Ethics Committee (permit number: KWS/BRM/5001).

During field surveys, animals were captured using standard small-mammal survey protocols, including Sherman live traps and museum snap traps, set along transects with 10-meter spacing between trap stations. We recorded external body measurements, including head–body length, tail length, hind-foot length, and ear length (all in mm), and body mass for each animal. Additionally, we prepared new museum specimens (skins and skulls) in the field, which were then deposited at the National Museums of Kenya (NMK) and the Kunming Institute of Zoology, Chinese Academy of Sciences (KIZ). Liver and muscle tissues were preserved in 99.6% ethanol at –80 °C at NMK, with duplicate samples transferred to KIZ. For detailed field-trapping and sample-preparation protocols, refer to the associated studies (Musila et al., 2019; Onditi et al., 2020, 2025).

DNA sequencing and sequence analysis

For new samples, we extracted total genomic DNA from liver and muscle tissues preserved at –80 °C in 99.6 % ethanol using the sodium dodecyl sulfate protocol. We sequenced the mitochondrial cytochrome b gene (*CYTB*) as a baseline marker for all the samples. The polymerase chain reaction (PCR) template contained genomic DNA, a primer pair, Power Taq Master Mix, and ultrapure water (Supplementary Table S2). The *CYTB* gene has an extensive comparative database in small mammals, which makes it ideal for continental phylogenetic reconstructions, and its evolutionary rate is appropriate for resolving species- and population-level divergences (Tobe et al., 2010). From the *CYTB* sequences, we subsampled the tissues to sequence six additional loci: two mitochondrial genes (D-loop and cytochrome-oxidase I [*COI*]) and four nuclear genes (recombination-activating gene 1 [*RAG1*], interphotoreceptor retinoid-binding

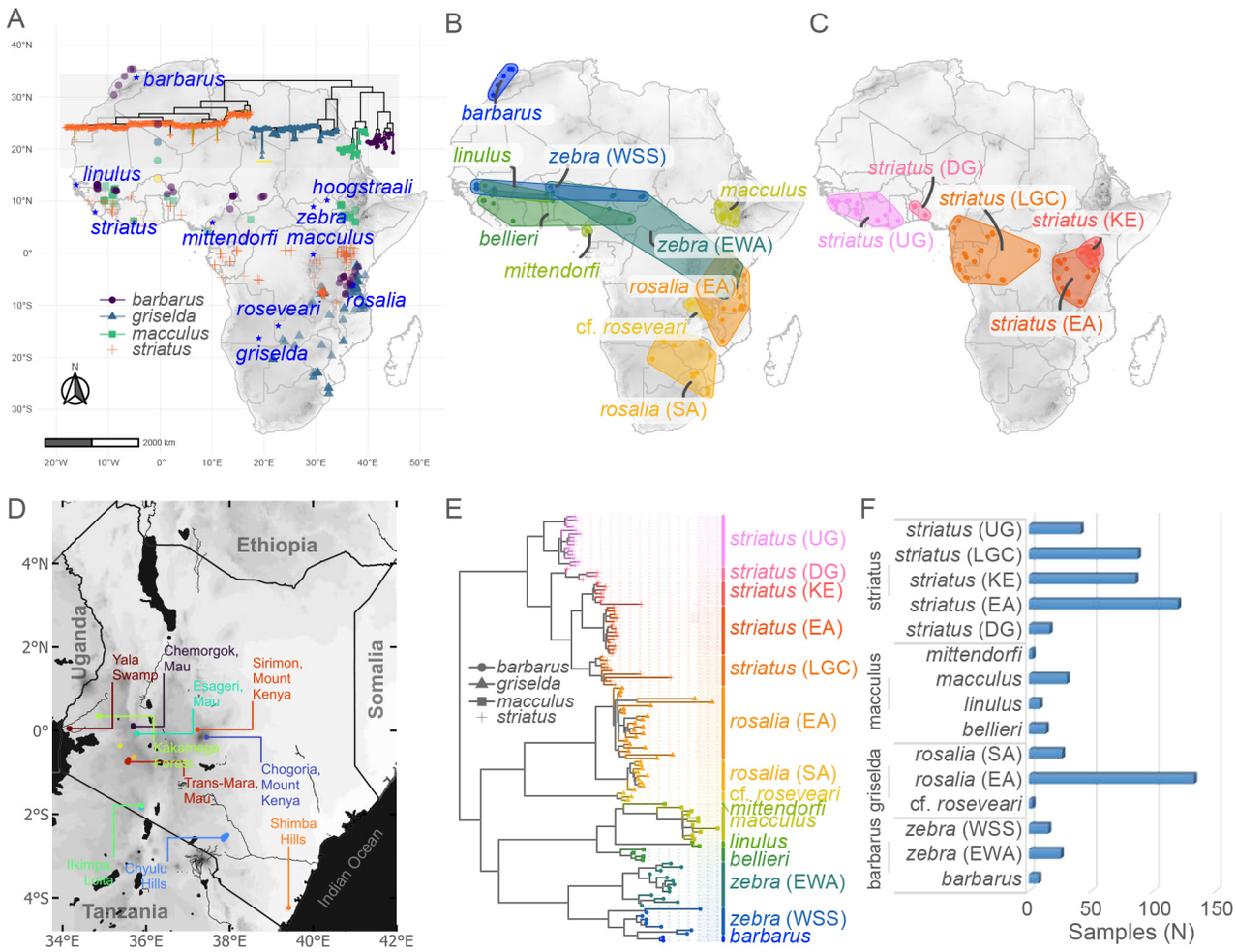

Figure 1 The geographical distribution and phylogenetic relationships of the *Lemniscomys* samples used in the study

A: The distribution of samples colored according to the four species groups with a schematic phylogenetic relationship in matching colors and symbols just above the map. B and C: The sampling points and bounding extents of MOTUs assigned to the *barbarus*, *griselda*, *macculus* (B), and *striatus* (C) species groups. D: The sampling sites of the new field surveys in Kenya. E: The mitochondrial cytochrome b (*CYTB*) phylogeny of samples colored in matching colors as the points and bounding extents in B and C. F: Sampling summary across the species groups and MOTUs on the y-axis and the number of samples on the x-axis.

protein [*IRBP*], 7-dehydrocholesterol reductase [*DHCR7*], transient-receptor-potential [*TRPV4*] and smoothened receptor [*SMO*]). The full thermocycling parameters for the PCR setup are summarized in Supplementary Table S2. We selected these loci for their demonstrated informativeness in mammalian systematics and their extensive representation in public databases (Agnarsson & May-Collado, 2008; Onditi et al., 2021, 2022). The resulting PCR products were sequenced bidirectionally on an ABI sequencer (Applied Biosystems, Waltham, MA, USA), and the chromatograms were de novo assembled and manually inspected in Geneious Prime® 2025.0.2 (www.geneious.com). To maximize taxon coverage, we downloaded the corresponding GenBank sequences (Supplementary Table S3). We BLAST-searched the new sequences in NCBI (https://blast.ncbi.nlm.nih.gov/; accessed on 30 September 2025) to verify their taxonomic identities. We then produced alignments using MAFFT v7 (Katoh & Standley, 2013) and compiled the mitochondrial, nuclear, and combined matrices into partitions using the SEGUI app v1.1.2 (Handika & Esselstyn, 2024). The resulting alignments included the mitochondrial alignment (*CYTB*, D-loop; 2,134 bp), the nuclear alignment (*RAG1, IRBP, SMO, TRPV4, DHCR7*; 3,968 bp), and the complete concatenated alignment combining the mitochondrial and nuclear matrices (53 sequences, 6,102 bp). We used the corresponding GenBank sequences of the African unstripped grass mice (*Arvicanthis niloticus*) as outgroups. The final *CYTB* alignment comprised 621 sequences: 95 newly sequenced and 526 GenBank sequences, representing all publicly available genetic material for this genus and spanning the currently recognized species, except *L. hoogstraali* and *L. griselda* (The American Society of Mammalogist's Mammal Diversity Database, 2025).

Phylogenetic analysis and species delimitation

We reconstructed phylogenetic relationships using maximum likelihood (ML) and Bayesian inference (BI) methods. Substitution models for these tests were selected in ModelFinder v2.1.1 using the Bayesian information criterion (BIC) (Kalyaanamoorthy et al., 2017), and the best model was selected based on the lowest BIC value (Supplementary Table S2). We implemented the ML analyses in IQ-TREE3 (Minh et al., 2020; Wong et al., 2025) with 5,000 ultrafast bootstrap replicates and a maximum of 1,000 iterations for branch support estimations. The BI analyses were performed in MrBayes for 100×10^6 Markov-chain Monte Carlo (MCMC) generations, with sampling every 5,000 steps. Analyses were

based on the *CYTB* dataset and three concatenated datasets: mitochondrial, nuclear, and complete concatenated alignment combined with the mitochondrial+nuclear matrix. We visualized, annotated, and drew the resulting trees in FigTree (http://tree.bio.ed.ac.uk/software/figtree/) and tvBOT (Xie et al., 2023).

For species delimitation, we used the *CYTB* alignment rather than the subsampled concatenated alignments because it was the most geographically and genetically representative of our combined sampling coverage and the corresponding ML and BI trees. First, to reduce sequence redundancy, we collapsed identical sequences into unique haplotypes with DnaSP v6.12.03 (Rozas, 2009). We then evaluated species limits using four complementary single-locus approaches: the ASAP (Assemble Species by Automatic Partitioning) (Puillandre et al., 2021, 2024), the OTU-picking branch-cutting method (bcut) (Mikula, 2018), the multirate Poisson tree processes (mPTP) model (Kapli et al., 2017), and the generalized mixed Yule–coalescent (GMYC) model (Fujisawa & Barraclough, 2013). ASAP partitions alignments into MOTUs based on pairwise genetic distances. We implemented the ASAP analysis in iTaxoTools (Vences et al., 2021). The GMYC and bcut delimitation were performed in R using the package 'splits' (Fujisawa & Barraclough, 2013) and the time-calibrated BI tree for the former and the 'branchcutting' R package (Mikula, 2018) and the ML tree for the latter. The mPTP method requires a nonultrametric phylogram with branch lengths in substitutions; therefore, we ran mPTP on a maximum-likelihood tree from the same alignment (Kapli et al., 2017).

Genetic and morphological diversity and population structuring

We quantified genetic diversity within and among *Lemniscomys* lineages with DnaSP. For each alignment, we calculated the number of polymorphic sites, total mutations, number of haplotypes (H), haplotype diversity (Hd), nucleotide diversity (π), mean pairwise differences (k), and neutrality statistics (Fu & Li's D* and F*, Tajima's D), retaining associated *P*-values. We generated haplotypes from both the new and GenBank sequences for downstream analyses. We also calculated pairwise Kimura 2-parameter (K2P) distances in MEGA v12 (Kumar et al., 2024) using the pairwise deletion method for gaps and ambiguous sites. We used median-joining networks generated in PopART v1.7 to explore genealogical relationships among MOTUs (Bandelt et al., 1999; Leigh and Bryant, 2015). High numbers of polymorphic sites, mutations, H, Hd, π, and k indicate divergent haplotypes and high genetic diversity, whereas low values suggest reduced diversity (Rozas et al., 2017). Strongly positive or negative neutrality statistics (Fu & Li's D*, F*, Tajima's D) with significant P values indicate departures from neutral mutation–drift equilibrium consistent with demographic change or selection, with nonsignificant values implying no strong evidence against neutrality and demographic stability (Korneliussen et al., 2013; Ramírez-Soriano et al., 2008; Rozas et al., 2017).

For the morphological analyses, external body measurements, including body mass and head–body, tail, hind foot, and ear lengths, were analysed together with cranial variables to identify diagnostic characters distinguishing MOTUs. We obtained samples from museum collections housed at the KIZ and NMK. From these, we measured craniodental variables on cleaned skulls following established protocols (Carleton & Van Der Straeten, 1997; Kawakami & Yamamura, 2008). From each skull, we recorded sixteen craniodental variables to the nearest 0.01 mm using a semi-digital caliper (Supplementary Figure S3). The resulting measurements were filtered to exclude outliers using the 1.5 IQR rule per MOTU, then log10-transformed to improve normality before analyses, and analyzed using principal component analysis and discriminant function analysis in PAST v5.0.2 (Hammer & Harper, 2024) or R v4.5.2 (The R Core Team, 2025).

Divergence analysis and ancestral range analysis

Molecular dating was performed in BEAST using the StarBEAST3 package, which samples gene trees and infers a species tree within a single Markov process (Douglas et al., 2022). We employed an uncorrelated lognormal relaxed clock, a Yule Model tree prior, and a GTR substitution rate model, and used taxon sets paralleling MOTUs. For divergence date constraints, *Lemniscomys,* like most African Rodents, lacks a detailed fossil record for reliable primary calibrations; therefore, we used secondary calibration points. We used three secondary calibration points based on Hánová et al., (2021) [the most recent common ancestor (MRCA) of *Lemniscomys* and *Arvicanthis* using fossil-based constraints from Mikula et al., (2021)]. These studies built on recent murid fossil discoveries and dating (Aghová et al., 2018), making their date estimates appropriate for our analysis of the divergence of the Arvicanthine lineage. Our three calibration points included: (i) The split between *Arvicanthis* and *Lemniscomys* constrained to a lower (2.5%) and upper (97.5%) highest posterior density (HPD) of 2.58 and 3.10, respectively, matching a log-space μ of 1.04 and a σ of 0.047 MRCA priors; (ii) The *Lemniscomys* MRCA was fixed to an HPD of 1.86–2.34, a log-space μ of 0.735, and a σ of 0.059; and (iii) We also constrained a ((*griselda*), (*striatus*, *macculus*)) MRCA to an HPD of 1.57–2.30, log-space μ of 0.642, and σ of 0.097 following Hánová et al. (2021)'s estimates. Two independent MCMC chains were run for 100 million generations, sampling every 5,000 steps; we discarded the first 10% of samples as burn-in, and checked convergence and effective sample sizes in Tracer v1.7.2 (Rambaut et al., 2018). We summarized the resulting BEAST trees as maximum clade credibility trees in TreeAnnotator (Rambaut & Drummond, 2024) and displayed them in FigTree and tvBOT.

For ancestral-range analysis, we used the time-calibrated species tree as input in BioGeoBEARS (Matzke, 2013a, 2013b, 2014). We compared three core models (DEC, DIVA-like, and BAYAREA-like) together with their '+J' extensions, which explicitly accommodate founder-event speciation at cladogenesis. For ancestral areas, we coded six climatically coherent macroregions that likely impacted *Lemniscomys* divergence and radiations (Behrends et al., 2024; Couvreur et al., 2021; Cuypers et al., 2022; Frost, 1996; Huhndorf et al., 2007; Huntley, 2023; Krásová et al., 2021; Linder et al., 2012; Pennington et al., 2004): (i) East Africa; the sky-island chain from the Kenyan and Tanzanian highlands through the Eastern Arc to northern Malawi, including the western Rift montane forests plus adjacent Congolian lowlands and the Rwenzori–Virunga moorlands; long-term montane refugia likely maintained stable microclimates through Pliocene–Pleistocene oscillations; (ii) Ethiopian highlands; endemic-rich montane forests, grasslands, and moorlands on the Horn of

Africa plateau; (iii) Upper Guinea; the Upper Guinea rainforest block and the lower Guinea coastal forests flanking the Dahomey Gap; (iv) Lower Guinea to central Congolian forests; with the Lower Guinea block acting as a connector between Upper Guinea and Central/East African montane systems, and the Dahomey Gap intermittently functioning as a savanna filter; (v) Zambezian; the Miombo-dominated woodland belt of central–southern Africa, facilitating north–south range dynamics during cooler, drier periods; and (vi) Mediterranean (Maghreb); the disjunct North African range where *Lemniscomys barbarus* occurs north of the Sahara.

Species distribution modeling and land cover change analysis

To evaluate whether biogeographic scenarios were consistent with environmental constraints, we implemented per-MOTU species distribution models (SDMs) assuming the continental extent was accessible to all MOTUs across modelled periods, since we could not assume niche conservatism in the deep-time projections. The SDMs were implemented in Maxent v3.4.1 (Phillips et al., 2006) using the georeferenced occurrence data. From the raw occurrences, we first implemented spatial rarefaction using the SDM toolbox 2.0 (Brown, 2014; Brown et al., 2017) to reduce sampling redundancy, leaving 311 occurrences for the modelling (Supplementary Table S4). In the MaxEnt modelling setup, we generated 10k background points, withheld 25% of the occurrences at random for testing, applied the maximum test sensitivity plus specificity rule to generate threshold-based habitat suitability maps and metrics (Liu et al., 2013), and used five bootstrap replicates to quantify uncertainty, using the average across the five replicates for the final analysis summaries. We used variable-response curves and jackknife tests to assess the importance of the predictors, and we computed the area under the receiver operating characteristic curve from the test data for each replicate to evaluate model performance. Spatial summarization and mapping were performed in R using terra, tidyterra (Hernangómez, 2023), and various tidyverse tools (Wickham et al., 2019). To aid interpretation and enable downstream metrics, continuous maps were thresholded using the maximum sensitivity plus specificity rule (Liu et al., 2013).

For environmental predictors, we used bioclimatic variables for the current period and projected models for paleoclimatic and future scenarios. The current (1981-2010) climate data were obtained from the CHELSA V2.1 bioclim dataset (Brun et al., 2022a, 2022b) (https://www.chelsa-climate.org/datasets/chelsa_bioclim; accessed on 5 April 2024) at a 30-arc-second (~1 km) resolution. Paleoclimate data were compiled from the Paleoclim database (Brown et al., 2018) (http://www.paleoclim.org/; accessed on 24 November 2024) at 2.5-arc-minute (~5 km) resolution, covering time periods from the late Pliocene to the Anthropocene. These included Marine Isotope Stage M2 (~3.3 Ma) simulations (Dolan et al., 2015), climate reconstructions for the last 21 kyr at regional and global scales (Fordham et al., 2017), last-interglacial Northern Hemisphere warming (Otto-Bliesner et al., 2006), Pliocene paleogeographic influences (Hill, 2015), and climate change during the Early Pleistocene and Pliocene (Brown et al., 2018). Future climate projections used CMIP6 data for SSP1-2.6, a low-emissions, sustainability pathway, and SSP5-8.5, a high-emissions, fossil-fuel pathway, covering the 2011–2040, 2041–2070, and 2071–2100 periods (Ocón et al., 2021). These future bioclimatic variables were also sourced from CHELSA V2.1 at 30 arc-seconds (~1 km). Across datasets, we obtained the standard set of 19 bioclimatic variables (Supplementary Table S5) as raster layers. These variables summarize annual means, seasonality, and climatic extremes in temperature and precipitation, which are key determinants of vertebrate diversity patterns and species' distributions across spatial and temporal scales (Elith & Leathwick, 2009). The layers were processed to a common spatial resolution and extent using the R package terra (Hijmans et al., 2024) to resample and align the layers. We then used correlation analysis to exclude highly correlated variables (Supplementary Figure S5).

We further quantified temporal and spatial changes in land-use/land-cover (LULC) within each MOTU range (the convex hull minimum bounding geometry that overlaps a MOTU's occurrence points). We obtained gridded, class-specific LULC raster data from Li et al., (2016). The layer reports the proportion of cover per 1 km cell (0–100%) for forest, shrub, grass, cropland, barren, wetland, water, impervious surface, urban green space, and snow/ice, from 2010 to 2100 under four representative concentration pathways (RCP 2.6, 4.5, 6.0, 8.5). We used the *terra* package in R to manage, align, and crop the multi-layer rasters to the genus range extent and to each MOTU range. We then computed MOTU-level, area-weighted mean proportional cover, and total area for each LULC class × year × scenario using the *exactextractr* package (https://cran.r-project.org/package=exactextractr), which computes zonal statistics efficiently while accounting for partial cell coverage at polygon boundaries.

We also overlaid MOTU ranges (convex hull minimum bounding geometry overlapping a MOTU's occurrences) over the Köppen–Geiger climate classification (Beck et al., 2023) to analyze relationships to temporal climate changes. The Köppen–Geiger climate classification system defines global climate types based on long-term monthly temperature and precipitation patterns, using seasonal and threshold criteria. It aligns these climatic zones with characteristic vegetation distributions (Kottek et al., 2006) and is widely used to explore the impacts of climate and associated ecosystem conditions (Chen & Chen, 2013; Klinges et al., 2025).

RESULTS

Species delimitation and phylogenetic reconstruction

The number of putative clusters recovered across methods ranged from 14 to 32 MOTUs (Figure 2). Across the four species-delimitation approaches (ASAP 19, GMYC 20, mPTP 32, and bcut 14), inferred MOTU numbers were broadly congruent, with all methods supporting the same major lineages and disagreeing on a subset of terminal clades where mPTP recovered additional splits relative to bcut, ASAP, and GMYC. We compared the resulting species partitions to derive a conservative, biologically interpretable consensus of 15 MOTUs (Figure 2). These 15 MOTUs represent nine named species spread across four previously supported species groups (posterior probability [PP] = 1.0; UFBoot ≥ 91): (i) the *barbarus* group (*L. barbarus* and *L. zebra* [two MOTUs]), (ii) the *griselda* group (*L.* cf. *roseveari* and *L. rosalia* [two MOTUs]), (iii) the *macculus* group (*L. bellieri*, *L. limulus*, *L. macculus*, *L. mittendorfi*), and (iv) the *striatus* group (*L. striatus* [five MOTUs]). Across the delimitation methods, there is strong concordance in recognizing all MOTUs, except the geographically structured forms of *L. striatus*, *L. rosalia,* and *L.*

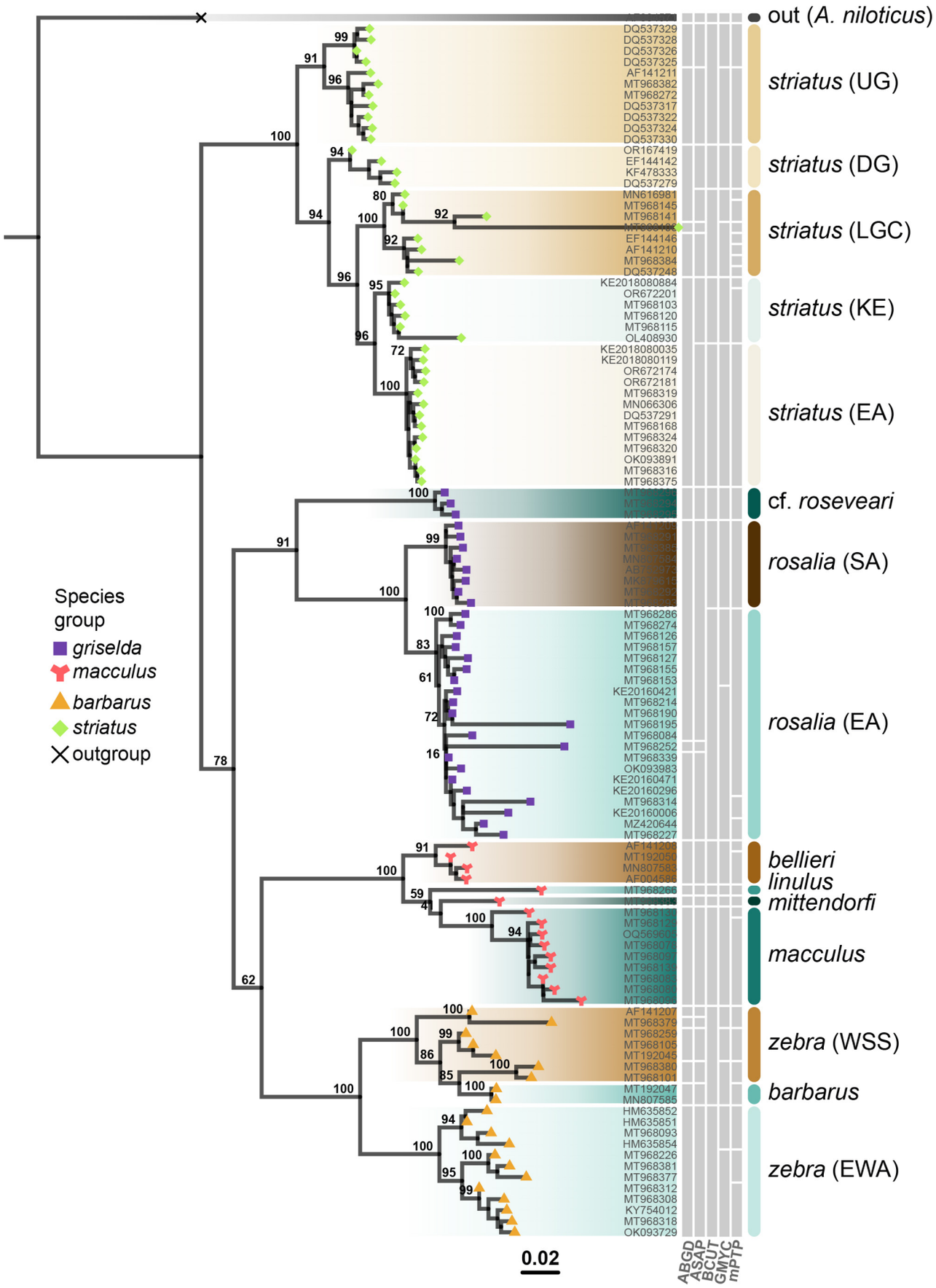

Figure 2 Maximum likelihood phylogenetic reconstruction of the genus *Lemniscomys* using the cytochrome b gene

The gray clade bars and labels indicate the partitioning schemes suggested by various species delimitation methods. The colored bars indicate the consensus scheme adopted as species units in the study.

cf. *roseveari*, which are split or lumped inconsistently across methods. From the *Lemniscomys* root, two main lineages diverged: a *striatus* clade and a clade containing the remaining three groups, within which *griselda* is sister to (*macculus*+*barbarus*) (Figure 2).

The spatial distribution of MOTUs mirrors the topology of phylogenetic relationships, such that geographic distance correlates positively with phylogenetic separation (Figure 1; Supplementary Figure S5). The *barbarus* group shows a north–south break, as *L. barbarus* is confined to the Maghreb (Morocco), whereas *L. zebra's* two MOTUs align with western (*zebra* WSS) versus a more easterly savanna belt across the Sahel–Sudanian (*zebra* EWA). The *griselda* group is centered in eastern and southern Africa, with cf. *roseveari* in East Africa and *L. rosalia* split into eastern- and southern-African MOTUs. The *macculus* group comprises west-central African endemics (*L. bellieri*, *L. limulus*, and *L. mittendorfi*) and an Ethiopian highlands MOTU (*L. macculus*). The *striatus* group contains five regionally cohesive MOTUs: Upper Guinea (*striatus* UG), Dahomey Gap (*striatus* DG), Lower Guinea–Congolian (*striatus* LGC), Kenya (*striatus* KE), and East Africa (*striatus* EA). We recovered these range–phylogeny correspondences with high node support (Supplementary Figures S1,2).

The new Kenyan survey samples clustered into three MOTUs (*rosalia* EA, *striatus* EA, and *striatus* KE) representing two nominal species, *L. rosalia* and *L. striatus* (Supplementary Figure S6). Among them, *rosalia* EA is from the Chyulu and Shimba Hills, *striatus* EA from Kakamega and the Mau Forest blocks, and *striatus* KE from Kakamega Forest, Mount Kenya, Loita Hills, Mau Forests, and Yala Swamp (Figure 1).

The concatenated mitochondrial and nuclear alignments retrieved relatively congruent MOTU relationships with those recovered in the *CYTB* and the complete alignment, albeit with low support across most nodes (Supplementary Figure S7).

Genetic and morphological diversity, and population structure

DNA polymorphism and neutrality statistics based on the *CYTB* dataset revealed high haplotype diversity across species groups (Hd >0.94) and relatively low nucleotide diversity (π = 0.025–0.077), with the highest values observed in the *barbarus* group and the lowest in the *griselda* group (Supplementary Table S6). Tajima's D values were negative for *griselda* and *striatus* but positive and nonsignificant for *barbarus* and *macculus*. We recorded large negative Fu's Fs values in the *striatus* MOTUs and the combined dataset. Among the MOTUs, we recovered between 3 and 40 haplotypes corresponding to overall high haplotype diversity ($\bar{x}$ Hd=0.892) and high divergence (π=0.077) (Supplementary Table S6, S7). The *zebra* MOTUs had the highest π (*zebra* EWA=0.035; *zebra* WSS=0.025), followed by the *striatus*-UG (π=0.02), whereas the *linulus* MOTUs presented the lowest diversity (Hd = 0.524; π=0.002). In the *striatus* complex, the eastern Africa MOTU retained many haplotypes (h=40) with moderate π (0.012), whereas the Kenya subset had a reduced Hd (0.758) and lower π (0.009). Neutrality tests were predominantly negative across populations (e.g., Tajima's D≤0 and strongly negative Fu's Fs in several groups, such as *striatus*-EA = −8.06 and *rosalia*-EA = −13.09) (Supplementary Tables S6, S7).

Evolutionary distances between MOTU pairs were lower within MOTUs (0.3% [*linulus*] to 3.8% [*zebra* EWA]) than between them (3.9% [*striatus* EA vs. *striatus* KE] to 18.4% [*barbarus* vs. *rosalia* SA]) (Table 1). The *barbarus* group was the most diverse (7.7%), followed by the *macculus (*6.2%), *striatus* (4.7%), and *griselda* (3.6%) groups, with between-group distances not significantly different (14.9–16.3%).

The median-joining haplotype network placed MOTUs into lineage- and geography-specific clusters (Figure 3). The *zebra* and *barbarus* MOTUs clustered distinctly from the *striatus* MOTUs, which formed a distinct grouping from all other species groups.

There was little external morphological partitioning tracking the genetic clusters, with most MOTUs clustered within the *L. striatus* morphotype, with notable craniodental differentiation between *striatus, rosalia,* and *linulus*, and no within-MOTU partitioning (Supplementary Figures S8, S9).

Table 1 Estimates of evolutionary divergence for sequence pairs within and between the molecular operational taxonomic units (MOTUs) identified in this study

MOTU	(b1)	(b2)	(b3)	(g1)	(g2)	(g3)	(m1)	(m2)	(m3)	(m4)	(s1)	(s2)	(s2)	(s3)	(s4)
(b1) *barbarous*	0.007	0.013	0.007	0.018	0.024	0.023	0.016	0.017	0.019	0.045	0.017	0.021	0.016	0.018	0.017
(b2) *zebra* (EWA)	0.100	0.03	0.013	0.019	0.024	0.021	0.018	0.020	0.020	0.048	0.018	0.019	0.017	0.019	0.017
(b3) zebra (WSS)	0.050	0.112	0.04	0.018	0.021	0.018	0.014	0.019	0.017	0.043	0.015	0.018	0.016	0.017	0.015
(g1) cf. *roseveari*	0.167	0.175	0.169	0.014	0.016	0.015	0.020	0.020	0.020	0.041	0.017	0.018	0.018	0.018	0.018
(g2) *rosalia* (EA)	0.156	0.166	0.153	0.125	0.011	0.008	0.019	0.026	0.024	0.039	0.021	0.021	0.019	0.021	0.018
(g3) *rosalia* (SA)	0.192	0.180	0.170	0.144	0.052	0.012	0.018	0.023	0.021	0.038	0.017	0.019	0.018	0.019	0.017
(m1) *bellieri*	0.138	0.159	0.143	0.174	0.154	0.158	0.013	0.014	0.013	0.022	0.015	0.017	0.016	0.017	0.017
(m2) *linulus*	0.139	0.162	0.153	0.164	0.171	0.165	0.089	0.004	0.013	0.024	0.020	0.020	0.020	0.018	0.019
(m3) *macculus*	0.148	0.166	0.151	0.173	0.168	0.170	0.083	0.086	0.012	0.037	0.018	0.021	0.020	0.018	0.018
(m4) *mittendorfi*	0.223	0.265	0.233	0.216	0.200	0.199	0.093	0.094	0.112		0.033	0.038	0.038	0.034	0.039
(s1) *striatus* (KE)	0.168	0.167	0.158	0.170	0.163	0.165	0.153	0.174	0.156	0.197	0.01	0.006	0.009	0.009	0.010
(s2) *striatus* (EA)	0.171	0.164	0.160	0.174	0.167	0.168	0.164	0.173	0.169	0.217	0.041	0.011	0.010	0.009	0.011
(s2) *striatus* (LGC)	0.140	0.150	0.138	0.161	0.139	0.157	0.160	0.164	0.162	0.229	0.059	0.064	0.017	0.009	0.009
(s3) *striatus* (DG)	0.164	0.171	0.157	0.168	0.152	0.172	0.168	0.161	0.146	0.198	0.062	0.066	0.061	0.012	0.010
(s4) *striatus* (UG)	0.153	0.154	0.143	0.161	0.147	0.154	0.157	0.158	0.158	0.217	0.075	0.078	0.075	0.071	0.021

Note: The lower diagonal displays the Kimura 2-parameter (K2P) distances, with corresponding error estimates in the upper diagonal; the diagonal shows the within-MOTU K2P distances. The analysis included 621 *CYTB* sequences, with pairwise deletions applied to ambiguous positions for each sequence pair. The cell color indicates the magnitude of distance in both diagonals, ranging from low (green) to high (red). We conducted the analysis using MEGA12 (Kumar et al., 2024). The corresponding DnaSP polymorphism and neutrality statistics are summarized in Supplementary Tables S6 and S7.

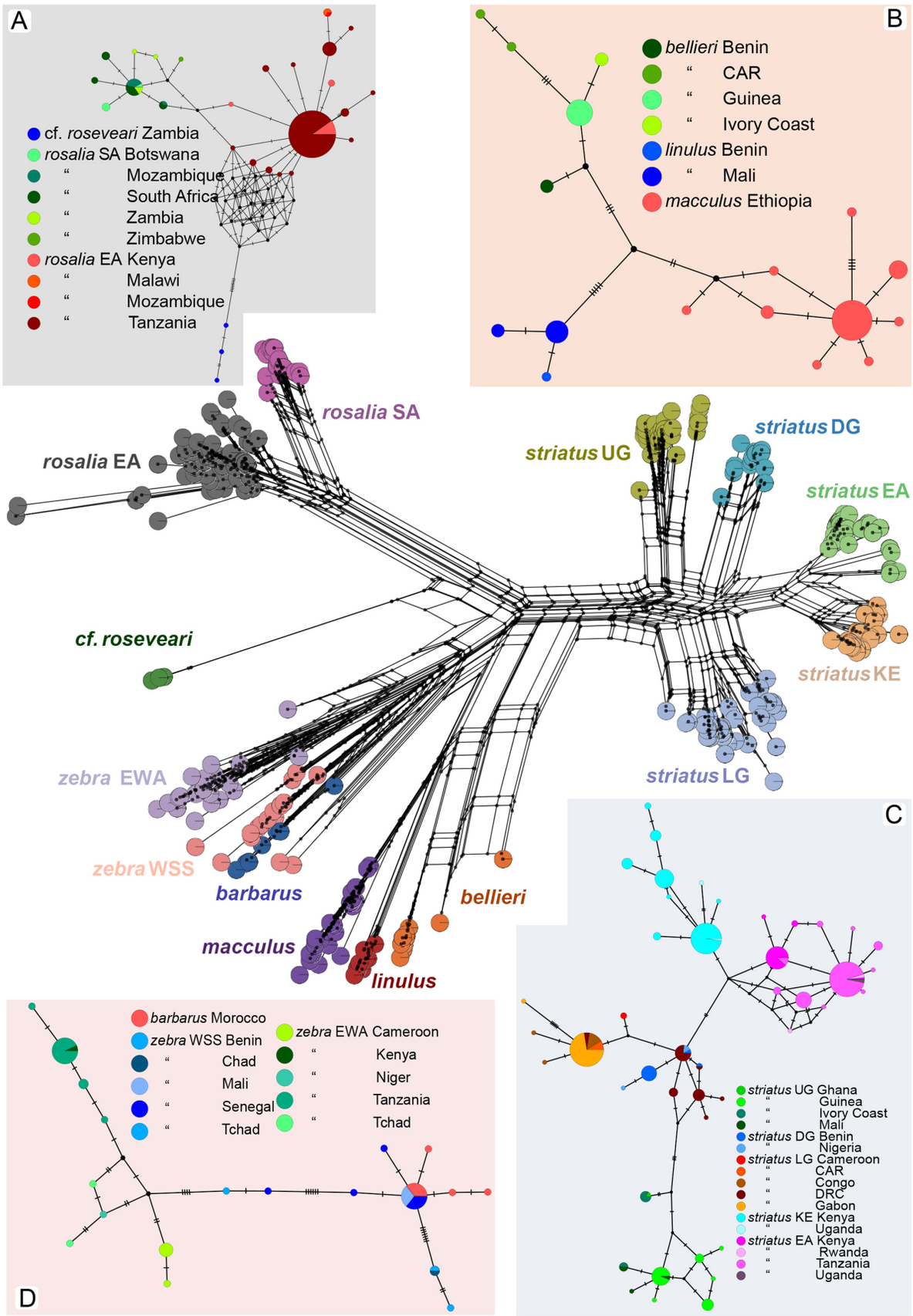

Figure 3 Population structure within and between the *Lemniscomys* MOTUs recovered in the study

The main backbone figure displays a phylogenetic network constructed from the unfiltered *CYTB* dataset, which served as the basis for the subsequent satellite haplotype network construction. Different color schemes in the backbone figure represent distinct MOTUs, while colors in the haplotype networks indicate sampling localities, as detailed in the corresponding legends. The quotation marks " indicate repeated species names with different geographic localities.

Divergence dating and historical biogeography reconstruction

The concatenated dataset recovered the split between *Lemniscomys* and *Arvicanthis* at 2.82 Ma (95% HPD: 2.57–3.07 Ma; PP=1.0) (Figure 4; Supplementary Table S8). Within *Lemniscomys*, the first split was the ancestor of the *barbarus* group at 2.11 Ma (95% HPD: 1.92–2.3 Ma; PP=1.0). Within-group divergence started between 0.5 Ma and 1.04 Ma, with splits leading to terminal MOTUs occurring between 1.04 Ma (*striatus* EA+*striatus* KE vs. other *striatus* MOTUs). The *CYTB* dataset recovered the split between *Lemniscomys* and *Arvicanthis* at 2.8 Ma (95% HPD: 2.51–2.90 Ma; PP=1.0). Within *Lemniscomys*, the common ancestor of the *striatus* MOTUs split from the ancestor of all other species groups at 2.2 Ma (95% HPD: 2.51–2.90 Ma; PP=1.0) (Figure 5). Within-group divergence occurred nearly simultaneously: *striatus*, *griselda*, and *barbarus* at 1.3 Ma, except for *macculus* at 1.1 Ma.

For both concatenated and *CYTB* datasets, DEC+J was the best-supported model (lowest AIC: weight 0.62–0.68), with the other +J models also reasonably supported, while all non-J models were disfavoured (*Δ*AIC ≥ 6.4–14.1) (Supplementary Table S9). Adding the founder-event speciation parameter j substantially improved likelihood (*Δ*LnL: +3.4 to +9.4) and reduced AIC (*Δ*AIC: −4.7 to −16.8) across all model families, and was consistently associated with lower estimated dispersal rates d and, where estimated, markedly lower extinction/range-contraction rates (Supplementary Table S9).

The best model suggested a West or Eastern African origin for *Lemniscomys*, followed by dispersal into northern, central, and southern Africa. Vicariance events bundled the four complexes across a savanna-forest mosaic that stretches from West Africa to the Rift and down into the Zambezian woodlands, and a northward jump into the Maghreb during humid phases, with at least one montane isolation event (Figure 5, Supplementary Figure S10). Early northward colonization to the Mediterranean gave rise to *L. barbarus*, with several eastward movements into East Africa, including the Ethiopian highlands (*L. macculus*), and southeastern dispersal into the Zambezian–South African region, producing *L. rosalia*. The *L. striatus* complex reflects a series of successive splits from West-Central African ancestors towards East African lineages, followed by regional diversification, including the Dahomey Gap and Lower Guinea MOTUs, with little evidence of back-dispersal once in East Africa. The *macculus* group (*L. bellieri*, *L. linulus*, *L. macculus*, and *L. mittendorfi*) likely originated from West Africa, including both crown splits (Supplementary Figure S10).

Species distribution modeling and land-use and land-cover changes

Species distribution models revealed broadly stable regional niches across past and future periods, punctuated by range contractions at peripheries rather than extensive displacement (Figure 6). The current predictions align well with the training data, supporting the model's adequacy (Supplementary Table S10).

The West and Central African MOTUs (*L. zebra*, *L. bellieri*, *L. linulus*) consistently retain suitable habitats in the Guinean–Congolian forest belt, exhibiting contraction during glacial conditions and subsequent Holocene/postglacial re-expansion, with late-century projections indicating an increase in fragmentation along the forest–savanna ecotone (Figure 6; Supplementary Table S10). Suitable habitats for the Maghreb endemic *L. barbarus* remained restricted to the Mediterranean region over time but contracted toward coastal montane refugia by 2071–2100. The southern savanna *L. rosalia* retains suitability in the Zambezian–South African corridor, with only modest shifts. Narrowly occurring species, such as the Ethiopian highland species (*L. macculus*), remain

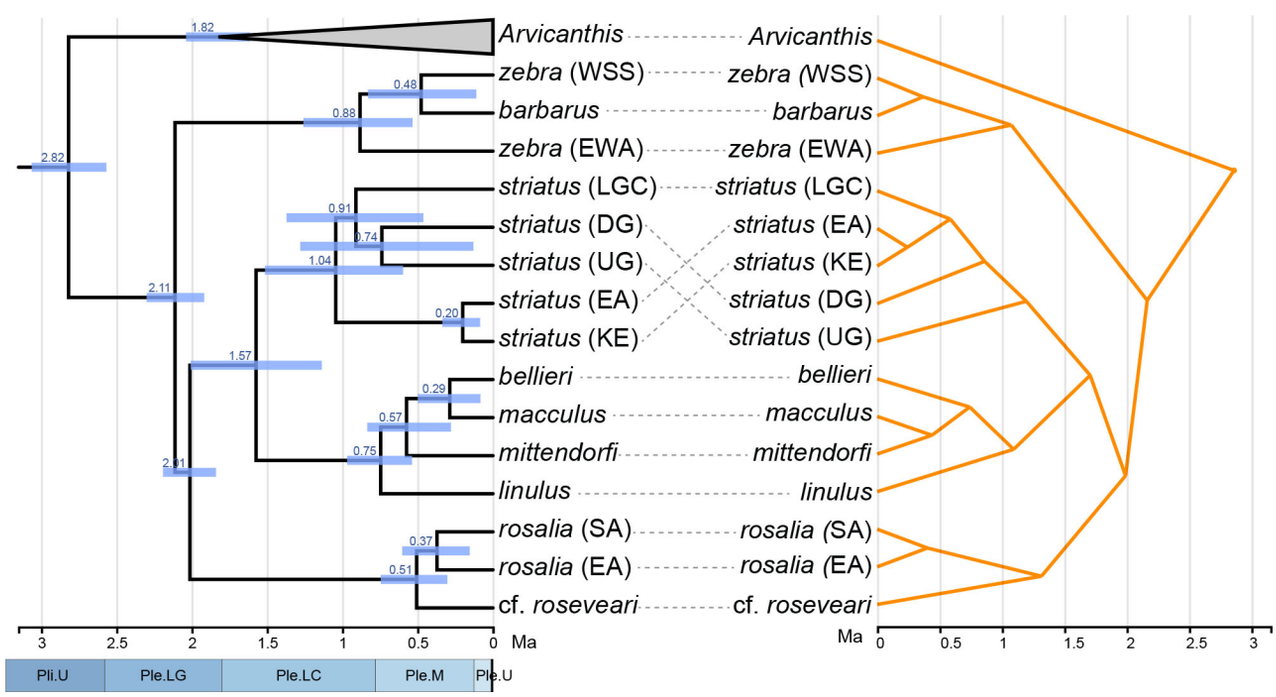

Figure 4 Divergence dating of the genus *Lemniscomys* based on the combined gene dataset (A) and the *CYTB* gene dataset (B)

The analysis, performed in starBEAST3, utilized the recovered MOTUs as taxon sets and the MRCAs of *Lemniscomys* and *Arvicanthis* as secondary calibration points. Ple.U: Upper Pleistocene, Ple.M: Middle Pleistocene, Ple.LC: Lower Pleistocene (Calabrian), Ple.LG: Lower Pleistocene (Gelasian), Pli.U: Upper Pliocene.

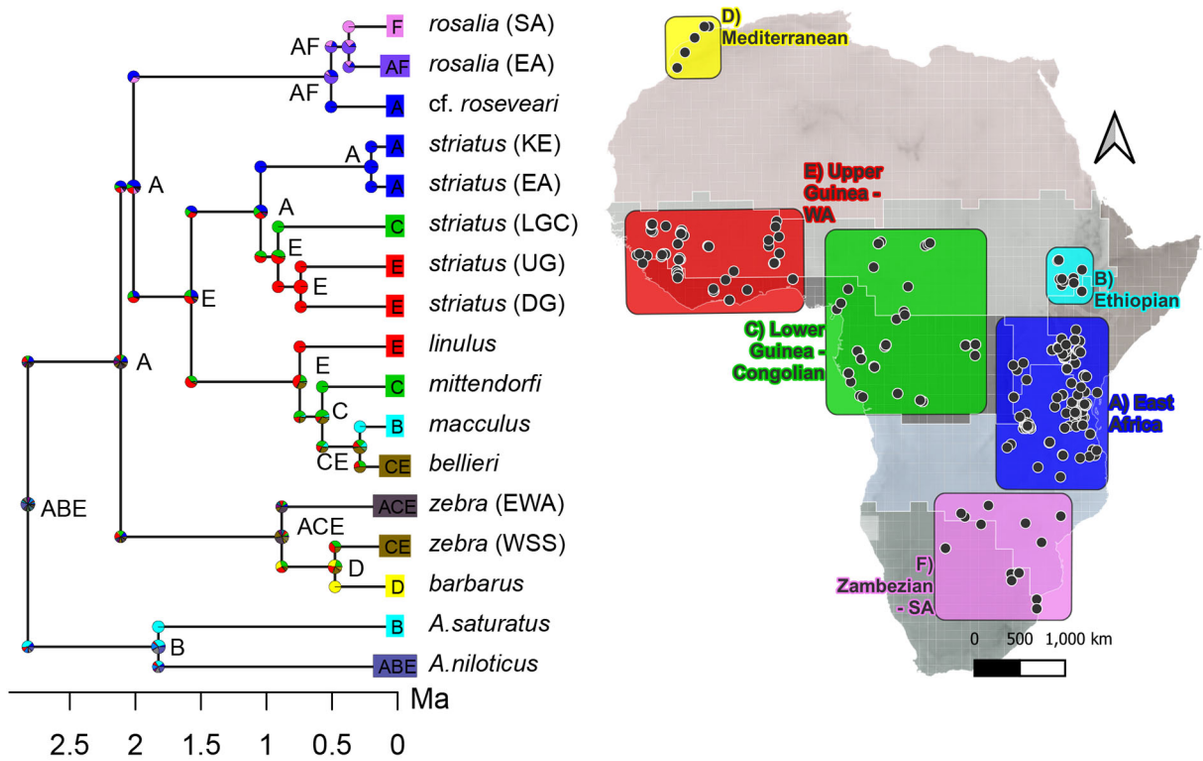

Figure 5 Ancestral area reconstruction for *Lemniscomys*

A time-scaled tree (left) with maximum-likelihood ancestral ranges shown by colored node symbols and tip letters; the map (right) shows biogeographic areas and sampled localities.

concentrated in montane habitats and show the greatest sensitivity to future warming (Supplementary Table S10). The widespread *L. striatus* complex maintains a west-to-east belt of suitability, with future models suggesting increased patchiness in East Africa. Notably, future trajectories diverge, with most species losing habitat between the current and mid-century estimates, whereas changes between the mid- and late-century estimates change negligibly (Figure 6; Supplementary Tables S10, S11).

MOTU range proportions across the Köppen-Geiger climate classes shifted across the 1900–2100 period, with the ranges generally shrinking or unchanging across the tropics, tropical savannas, and cold highlands, except for *rosalia* in tropical savannas and semi-arid steppes, and *striatus* EA and *striatus* UG in tropical savannas (Supplementary Figures S11, S12). Across the *Lemniscomys* range, the tropical rainforest consistently contracted between 1961 and 2020, and the hot-steppe and hot-desert expanded (Supplementary Figure S13). By 2041–2070, rainforest cover could decline by nearly half, with the late century extending this decline further as croplands and impervious surfaces proliferate (Supplementary Figure S13).

DISCUSSION

By integrating a multilocus dataset with morphometric data, our study considerably refines current understanding of the striped grass mice genus (*Lemniscomys*) systematics, evolutionary radiation, and interactions with changing climates and human landscapes. We identified 15 MOTUs corresponding to nine named species, with three of these species showing cryptic genetic subdivision. *Lemniscomys* diverged from its sister genus *Arvicanthis* approximately 2.8 Ma, likely within the Sudanian savanna belt, with most diversification occurring during the early to mid-Pleistocene. Across paleoclimatic, contemporary, and future climate scenarios, *Lemniscomys* lineages retained suitable habitat, suggesting considerable resilience or ecological flexibility to shifting environments over evolutionary timescales. These results sharpen the integrative phylogeographic framework for the genus and underscore the need for formal taxonomic reassessment of several classical lineages in light of genomic evidence that stabilizes morphospecies boundaries.

Overview of *Lemniscomys* species diversity and distribution

The phylogenetic results concur with recent studies focused on this genus and reinforce the need for an integrative taxonomic revision that combines genetics and morphology, a task that was not feasible in the current study for lack of access to critical type material. The recovered phylogenetic topology is concordant with the multilocus phylogeny of Hánová et al. (2021), but adds some novel changes in MOTU boundaries. For example, our 15 MOTUs are one fewer than those reported by Hánová et al., (2021); as we merged their far Upper Guinea MOTUs (*striatus* A and B) into a monophyletic unit (*striatus* UG). Taken together, our results have clear taxonomic implications, particularly when contrasting the broadly phylogenetically informative *CYTB*-only topology with the concatenated multilocus phylogeny. However, in the absence of MOTU-level morphological diagnosis, we are not in a position to robustly argue for or against the taxonomic updates proposed by Hánová et al., (2021) and instead focus our interpretation on evolutionary radiation patterns and their links to past, contemporary, and future climate change and anthropogenic impacts.

The divergence depths observed among MOTUs, which exceed typical intraspecific variation and align more closely

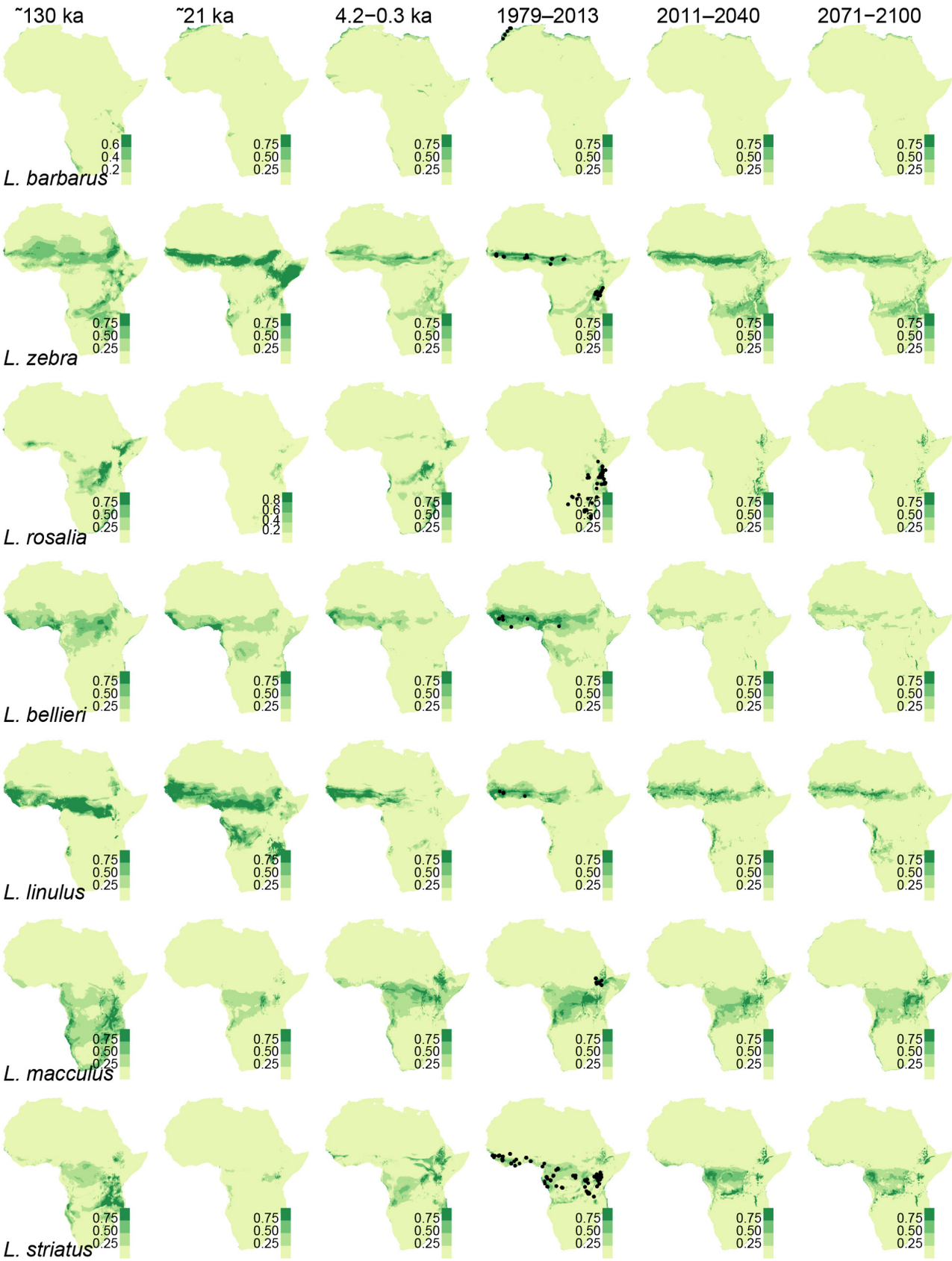

Figure 6 Species distribution models (SDMs) projecting past, contemporary, and future habitat distributions of *Lemniscomys* species

We implemented the analysis using the georeferenced genotyped (mitochondrial cytochrome b (*CYTB*)) samples used in the study. Each row represents a species-level collapse of the molecular operational taxonomic units (MOTUs) recovered in the study, and each column represents a time period. Shading denotes continuous habitat suitability (low–high), and black points in the '1979–2013' time slice column are the georeferenced genotyped occurrences used to calibrate the SDMs. See Supplementary Tables S10 and S11 for MOTU-level summaries of area change across periods and model performance.

with interspecific thresholds defined by contemporary species-concept frameworks (Baker & Bradley, 2006; Farias et al., 2001; Irwin et al., 1991; Tobe et al., 2010). Such divergence warrants further studies focused on formally elevating them to species status or an attempt to assess their boundaries in light of expanded and integrated genetic, morphological, and geographic sampling (De Queiroz & Gatesy, 2007).

The *Lemniscomys* range spans nearly the full breadth of sub-Saharan Africa with the outlier Barbary species *L. barbarus*. This distribution pattern suggests these species have broad ecological tolerance, spanning generalists thriving across diverse rainfall regimes, to 'island-like' specialists in single mountains. Encompassed in the recovered MOTUs, three wide-ranging generalists dominate. First, *L. striatus,* which traverses the humid–mesic Guineo-Congolian and Zambezian savannas from Guinea-Bissau East to western Kenya and south to Angola, D.R. Congo, Zambia, Tanzania, and Malawi, with outliers northward into Sudan and Ethiopia. Second, *L. zebra,* which essentially replaces *L. striatus* in drier Sahelo-Sudanian grasslands in an almost continuous west–east band from Senegal to Eritrea and extends south into much of East Africa to at least southern Tanzania. Third, *L. rosalia,* which favors the moister miombo/woodland mosaics from Kenya south to northeastern South Africa and west to southern Angola and northern Namibia (Monadjem et al., 2015; The American Society of Mammalogist's Mammal Diversity Database, 2025; Wilson et al., 2017). Encircling these generalists are localized endemics that underscore strong biogeographic compartmentalization as in other African rodents (Bryja et al., 2014a, 2014b; Mikula et al., 2021): *L. macculus* occurs from the Albertine Rift into East Africa and parts of West Africa; *L. bellieri* and *L. linulus* in the Upper Guinean block west of the Dahomey Gap; and *L. mittendorfi* is a cool-climate montane endemic confined to Mt. Oku, Cameroon. In the Maghreb, *L. barbarus* persists as a narrow coastal relict north of the Atlas in Morocco, Algeria, and Tunisia. Central–southern Africa hosts two near-endemics: *L. griselda* (Angola, adjoining the D.R. Congo, and NW Zambia) and the range-restricted *L. roseveari* (NW Zambia, possibly also found in Angola). The elusive *L. hoogstraali* is known only from its White Nile-type locality in northeastern South Sudan, which could reflect either point-endemism along the riparian corridor it supposedly inhabits or a chronic difficulty in observing and capturing it in the field. The East African MOTUs exhibit phylogeographic structures consistent with connections among adjacent savanna blocks and with barriers associated with rift systems (Bryja et al., 2014a, 2014b; Onditi et al., 2021), as illustrated primarily by the *L. striatus* MOTUs, which appear to mirror historical landscape connectivity and breaks (Dommain et al., 2022; Nicolas et al., 2008).

Notably, among the delimited 15 MOTUs, slightly different numbers and placements of MOTU boundaries between the delimitation methods are expected, as methods such as GMYC and related threshold approaches can oversplit population structure under particular tree shapes, sampling schemes, and demographic scenarios (Fujita et al., 2012; Luo et al., 2018). The integrative consensus we adopted, in which only lineages supported by multiple methods and forming cohesive, geographically structured clades in the multilocus phylogeny were recognized as MOTUs, avoids taxonomic inflation while retaining biologically meaningful structures (Fujita et al., 2012).

Evolutionary history of *Lemniscomys*

The 2.8 Ma (95% HPD 2.51–2.90 Ma) split between *Lemniscomys* and *Arvicanthis* we recovered aligns with recent estimates (Hánová et al., 2021; Mikula et al., 2021). Like other Arvicanthine species (Mikula et al., 2021), speciation in most *Lemniscomys* lineages occurred during the climatically unstable late Pliocene–Early Pleistocene. The early emergence of the *barbarus* species group supports the idea that, for these rodents, Pliocene–Pleistocene arid–humid oscillations alternately fragmented populations into refugia (Bibi & Kiessling, 2015; Cohen et al., 2022; deMenocal, 2004; Gibernau & Montuire, 1996). These alternations promoted allopatry as open habitats expanded, yielding the pulsed diversification pattern observed across multiple African rodents (Aghová et al., 2017; Bryja et al., 2010; Colangelo et al., 2013; Dobigny et al., 2013; Hánová et al., 2021; Onditi et al., 2021). The *Lemniscomys* split from other Arvicanthines also coincided with the onset of intensified orbital-scale climate oscillations that brought cooler, drier, more heterogeneous landscapes across Africa (Potts & Faith, 2015; Trauth et al., 2005). Moreover, open habitat expansion accelerated during this interval (Ségalen et al., 2007), whereas lake-level cyclicity in the East African Rift peaked (Trauth et al., 2007). These events could have facilitated habitat turnover, favoring allopatric diversification in refugia within *Lemniscomys,* mirroring the conclusions of other African rodent evolutionary studies (Mikula et al., 2021; Missoup et al., 2016; Onditi et al., 2021).

The ancestral range reconstruction placed the *Lemniscomys* crown ancestor in the Sudanian savanna (Burgess et al., 2004). Three of the four major lineages remain centered in West Africa. In contrast, eastward expansions by the *striatus*, *macculus,* and *zebra* complexes are comparatively recent, and restricted mainly to ecologically analogous savanna mosaics rather than forest biomes. These patterns align with savanna fragmentation around the Plio–Pleistocene boundary, which earlier studies invoked to explain parallel splits in *Arvicanthis* (Belmaker, 2018) and other murines (Lecompte et al., 2008). The restricted distribution of *macculus* along Guinean–Savanna ecotones (Denys et al., 2020) and the apparent competitive exclusion of *striatus* from southeastern Africa, where the *griselda* lineage colonized (Hánová et al., 2021), further illustrate how local ecological filters, rather than long-distance dispersal across dissimilar biomes, govern lineage sorting within *Lemniscomys*. Overall, the Plio–Pleistocene radiation of *Lemniscomys* appears to have been driven by short-range vicariance in West and Central Africa punctuated by episodic founder–event dispersals northward, eastward, and southeastward.

Climate change and anthropogenic impacts on spatialtemporal habitat changes

Lemniscomys showed a consistent association with open and mosaic biomes, including the Sahelian/Sudanian and Somali–Masai grasslands, and the more expansive Zambezian complex, while largely avoiding hyperarid cores and dense rainforest interiors. This biogeographic scenario aligns with the history of the tribe Arvicanthini in the late Miocene, when the spread of C4 grasslands and fragmentation of pan-African forests created both habitat corridors and new ecotonal opportunities for open-habitat murines (Mikula et al., 2021). The modeled, belt-like suitability

ribbons around the Congo Basin through time are therefore consistent with expectations from the clade's macroevolutionary setting, and the temporal slices we selected provide a mechanistic link to these patterns. During the last interglacial period, greener Saharan conditions and a northward rain belt likely permitted transient northward connectivity. By the LGM, cooling and drying favored southward and eastward displacement and fragmentation of suitable open habitats. The late Holocene conditions then led to the waning of the African humid period and the re-expansion of desert barriers (deMenocal et al., 2000). Our maps mirror *Lemniscomys'* macroevolutionary correlates of these changes, including thinning and shifts in suitability belts. In the contemporary climate baseline and future projections, modeled suitability shifts emphasize human-driven landscape changes will likely maintain or even expand suitability for some disturbance-tolerant *Lemniscomys* lineages (García-Peña et al., 2021).

In the *barbarus* group, suitable regions for *L. barbarus* remain constrained to the Maghreb–Mediterranean margin over time, consistent with its current biogeography and limiting its potential future range expansion under warming, given coastline-bounded habitats. For this species, the historical North African windows implied by interglacial greening do not reemerge in late-century projections, underscoring the enduring roles of Mediterranean aridity and coastal topography as filters. On the other hand, the wider-ranging Sahelian–Sudanian suitable habitat of *L. zebra* declined with Holocene aridification and modern land conversion, suggesting that for this species, East–West connectivity depends on maintaining ecotonal mosaics rather than continuous forests.

In the *griselda* group, *L. rosalia* habitat suitability centered on forest–savanna ecotones along the Congo margin and into East Africa, consistent with a lineage that avoids deep forest but benefits from edge dynamics. The Late-Holocene aridification and ongoing deforestation (Maley et al., 2018; Marchant et al., 2009) plausibly generate the reconstructed narrow strip of suitable areas, with mid-century futures indicating increased patchiness unless ecotones persist. Although we did not include *L. roseveari* in these models, it likely still occurs in suitable habitats in northwestern Zambia. Among the *macculus* group representatives, the emerging picture reinforces Rift- and highland-structured habitat tracking, with *L. macculus* and *L. linulus* showing broader east/northeast African belts that contract under LGM conditions and re-expand with late-Holocene and contemporary climates, whereas *L. bellieri* appears patchier. Finally, the *striatus* complex exhibits the most extensive contemporary suitability across the Sahelian/Sudanian and Zambezian belts, with projections indicating resilience in human-modified mosaics but emerging fragmentation at forest and desert edges, expected of such broadly occurring lineages (Mace et al., 2010; Stork et al., 2009).

The climate–LULC and SDM narrative reinforced the picture emerging from the phylobiogeographic reconstructions. High-suitability areas for *Lemniscomys* tracked the persistence of warm- season rainfall regimes across Africa's open biomes. Recent climate transitions will likely reorganize around tropical savannas, with limited encroachment by desert classes, consistent with projections of robust warming and modest, but regionally heterogeneous, precipitation changes (Knoke et al., 2023; Pirani et al., 2024). Within the Mediterranean offshoot (*L. barbarus*), the Maghreb area indicates the long-term persistence of warm-temperate dry-summer classes adjacent to arid zones, conditions matching the continuing coastal confinement inferred from the SDMs (Knoke et al., 2023). Land-use change trajectories across the genus range, such as rising cropland/impervious fractions and dynamic shrub/grass mosaics in several subregions, imply that early-successional agricultural landscapes may locally sustain disturbance-tolerant lineages, whereas forest loss and infrastructure growth increase fragmentation risk elsewhere (Banks-Leite et al., 2020; Franklin et al., 2016). Moreover, the narrow-range MOTUs are restricted to narrow highland distributions, making them particularly sensitive to climate change impacts and human activity, echoing the need to safeguard elevational connectivity, refugial areas, and key montane corridors in conservation planning.

Ecological and zoonotic implications of *Lemniscomys* phylogeography

The highly diurnal and prominent longitudinal stripes that *Lemniscomys* species feature are typically associated with visually mediated camouflage and a ground-dwelling, daytime lifestyle (Lahmam et al., 2008; Staps et al., 2023) and variations in predation risk and exposure (Schradin, 2008); which may impact mitochondrial gene expression and oxidative phosphorylation, with long-term predator-induced stress potentially influencing the mtDNA phylogenetic variation patterns (Kokkinopoulou & Moutsatsou, 2021). Nonetheless, in our *Lemniscomys* dataset, the primary phylogeographic pattern is best explained by historical demography and landscape connectivity, and the influence of predator-driven selection, diurnality, or striped fur on mtDNA structure remains speculative and outside the main scope of this study.

Several *Lemniscomys* species have been identified as potential reservoirs or incidental hosts of zoonotic agents in sub-Saharan Africa. Bacterial and protozoan pathogens, including Anaplasma, Bartonella, Coxiella, Leptospira, Trypanosoma, Plasmodium, and Borrelia, have been detected in *Lemniscomys striatus* and *L. zebra*, with the widespread *L. striatus* also listed among the species involved in plague foci in East Africa (Mangombi et al., 2021; Mbou-Boutambe et al., 2025). Recent studies on virome and targeted virus discovery have also reported novel orthonairoviruses, mammarenaviruses, and other RNA viruses associated with *Lemniscomys* hosts, including *L. striatus* and *L. rosalia*, highlighting their potential role in sylvatic transmission cycles (Kuhn et al., 2025; Ozeki et al., 2022). Our phylogeographic analyses reveal clear regional population structure and distinct ranges among the *Lemniscomys* MOTUs, with some lineages exhibiting broad distributions while others are geographically restricted. The well-connected MOTUs could facilitate the spread of pathogens. In contrast, strongly structured lineages might limit pathogen circulation to specific areas (Han et al., 2020; Mawanda et al., 2020). Although we did not test for infections in the current study, the spatial genetic framework provided here can guide future targeted surveillance and help incorporate host phylogeography into more mechanistic models of zoonotic risk involving *Lemniscomys* and co-distributed rodents.

CONCLUSION

Our study extends the integrative phylogeographic work on the genus *Lemniscomys*, supplementing recent genetic and

taxonomic conclusions and providing species-level phylogeographic insights. Taxonomically, our findings confirm the currently recognized species while highlighting the need to formally reassess the limits of several classically defined lineages in light of genus-wide genetic evidence to match morphospecies to their stable taxonomic placements across sampling depths. The pronounced divergences we detected within *L. striatus*, *L. rosalia*, and *L. zebra* suggest cryptic diversity or incipient evolutionary lineages that have not yet fully stabilized as distinct species. Earlier foundational treatments of *Lemniscomys* anticipated such heterogeneity and cautioned against conferring species status without integrative support; our results reinforce that prudence. As with many African small-mammal groups, we were unable to examine all critical types and comparative material needed for a formal taxonomic act; consequently, we recommend targeted revisionary work for future studies. Ecologically, species distribution models and our explorations of climate and land-use/land-cover changes suggest that *Lemniscomys* may be relatively buffered from climatically driven habitat loss, likely because of their frequent occurrence in broadly suitable, nonspecialized habitats. While this is a positive element from a species conservation perspective, such ecological flexibility complicates public health preparedness and zoonotic surveillance. In the event of outbreaks, populations that can shift among landscapes may be more complex to anticipate and contain. By integrating extensive geographic sampling with robust systematics, phylogeography, and habitat-suitability analyses, we provide a genus-wide framework to underpin future taxonomic revisions and conservation assessments across its pan-African range. We also offer broader insight into African faunal biogeography and how it is shaped by climate change and escalating human pressures.

SCIENTIFIC FIELD SURVEY PERMISSION INFORMATION

The animal handling procedures in these new field surveys adhered to Kenya's wildlife research regulations and the established guidelines for the use of wild animals in academic research (Sikes & The Animal Care and Use Committee of the American Society of Mammalogists, 2016; Underwood & Anthony, 2020). The research was approved by the Kenya Wildlife Service Research and Ethics Committee (permit number: KWS/BRM/5 001).

DATA AVAILABILITY

The novel DNA sequences have been deposited in GenBank under accession numbers PX756915 – PX757006.

SUPPLEMENTARY DATA

The article's supplementary data are available online.

COMPETING INTERESTS

The authors declare that they have no competing interests.

AUTHOR CONTRIBUTIONS

B.A.S: Conceptualization, methodology, formal analysis, investigation, resources, data curation, writing (original draft & review and editing). S.M.O.: Conceptualization, methodology, resources, data curation, writing (review and editing). S.W.H.: Resources, data curation, writing (review and editing). S.M.: Methodology, resources, writing (review and editing). Q.L.: Methodology, resources, writing (review and editing). Z.Z.C.: Methodology, resources, writing (review and editing). W.Y.S.: Methodology, resources, writing (review and editing). X.Y.L.: Methodology, resources, writing (review and editing). K.O.O.: Conceptualization, methodology, investigation, resources, writing (review and editing), supervision. X.L.J.: Conceptualization, methodology, investigation, resources, (review and editing), supervision, project administration, funding acquisition. All authors read and approved the final version of the manuscript.

ACKNOWLEDGMENTS

The mammal surveys and fieldwork in Kenya were carried out by teams from the National Museums of Kenya and the Kunming Institute of Zoology, Chinese Academy of Sciences, and we are very grateful for their logistical support. This research was funded by the Sino-Africa Joint Research Centre, Chinese Academy of Sciences (grant number: SAJC202402).

REFERENCES

Aghová T, Kimura Y, Bryja J, et al. 2018. Fossils know it best: Using a new set of fossil calibrations to improve the temporal phylogenetic framework of murid rodents (Rodentia: Muridae). *Molecular Phylogenetics and Evolution*, **128**: 98–111.

Aghová T, Šumbera R, Piálek L, et al. 2017. Multilocus phylogeny of East African gerbils (Rodentia, *Gerbilliscus*) illuminates the history of the Somali-Masai savanna. *Journal of Biogeography*, **44**(10): 2295–2307.

Agnarsson I, May-Collado LJ. 2008. The phylogeny of Cetartiodactyla: the importance of dense taxon sampling, missing data, and the remarkable promise of cytochrome *b* to provide reliable species-level phylogenies. *Molecular Phylogenetics and Evolution*, **48**(3): 964–985.

Baker RJ, Bradley RD. 2006. Speciation in mammals and the genetic species concept. *Journal of Mammalogy*, **87**(4): 643–662.

Bandelt HJ, Forster P, Röhl A. 1999. Median-joining networks for inferring intraspecific phylogenies. *Molecular Biology and Evolution*, **16**(1): 37–48.

Banks-Leite C, Ewers RM, Folkard-Tapp H, et al. 2020. Countering the effects of habitat loss, fragmentation, and degradation through habitat restoration. *One Earth*, **3**(6): 672–676.

Beck HE, McVicar TR, Vergopolan N, et al. 2023. High-resolution (1 km) Köppen-Geiger maps for 1901–2099 based on constrained CMIP6 projections. *Scientific Data*, **10**(1): 724.

Behrends GJ, Meheretu Y, Manthey JD. 2024. The Great Rift Valley is a more pronounced biogeographic barrier than the Blue Nile Valley for six Ethiopian Highland passerines in the eastern Afromontane biodiversity hotspot. *Ornithology*, **141**(4): ukae030.

Belmaker M. 2018. Criteria for identifying the African origin of early Pleistocene mammalian fauna in Eurasia. *Comptes Rendus Palevol*, **17**(4-5): 262–275.

Bibi F, Kiessling W. 2015. Continuous evolutionary change in Plio-Pleistocene mammals of eastern Africa. *Proceedings of the National Academy of Sciences of the United States of America*, **112**(34): 10623–10628.

Brown JL. 2014. SDMtoolbox: a python-based GIS toolkit for landscape genetic, biogeographic and species distribution model analyses. *Methods in Ecology and Evolution*, **5**(7): 694–700.

Brown JL, Bennett JR, French CM. 2017. SDMtoolbox 2.0: the next generation Python-based GIS toolkit for landscape genetic, biogeographic and species distribution model analyses. *PeerJ*, **5**: e4095.

Brown JL, Hill DJ, Dolan AM, et al. 2018. PaleoClim, high spatial resolution paleoclimate surfaces for global land areas. *Scientific Data*, **5**(1): 180254.

Brun P, Zimmermann NE, Hari C, et al. (2022a-06-13). CHELSA-BIOCLIM+ A novel set of global climate-related predictors at kilometre-resolution. EnviDat. https://doi.org/10.16904/envidat.332.

Brun P, Zimmermann NE, Hari C, et al. 2022b. Global climate-related predictors at kilometer resolution for the past and future. *Earth System Science Data*, **14**(12): 5573–5603.

Bryja J, Granjon L, Dobigny G, et al. 2010. Plio-Pleistocene history of West African Sudanian savanna and the phylogeography of the *Praomys daltoni* complex (Rodentia): the environment/geography/genetic interplay.

Molecular Ecology, **19**(21): 4783–4799.

Bryja J, Mikula O, Patzenhauerová H, et al. 2014a. The role of dispersal and vicariance in the Pleistocene history of an East African mountain rodent. *Praomys delectorum. Journal of Biogeography*, **41**(1): 196–208.

Bryja J, Mikula O, Sumbera R, et al. 2014b. Pan-African phylogeny of *Mus* (subgenus *Nannomys*) reveals one of the most successful mammal radiations in Africa. *BMC Evolutionary Biology*, **14**(1): 256.

Burgess N, Hales JDA, Underwood E, et al. 2004. Terrestrial Ecoregions of Africa and Madagascar: A Conservation Assessment. Washington: Island Press.

Carleton MD, Van Der Straeten E. 1997. Morphological differentiation among Subsaharan and North African populations of the Lemniscomys barbarus complex (Rodentia: Muridae). *Proceedings of the Biological Society of Washington*, **110**(4): 640–680.

Chen DL, Chen HW. 2013. Using the Köppen classification to quantify climate variation and change: an example for 1901–2010. *Environmental Development*, **6**: 69–79.

Cohen AS, Du A, Rowan J, et al. 2022. Plio-Pleistocene environmental variability in Africa and its implications for mammalian evolution. *Proceedings of the National Academy of Sciences of the United States of America*, **119**(16): e2107393119.

Colangelo P, Verheyen E, Leirs H, et al. 2013. A mitochondrial phylogeographic scenario for the most widespread African rodent. *Mastomys natalensis. Biological Journal of the Linnean Society*, **108**(4): 901–916.

Couvreur TLP, Dauby G, Blach-Overgaard A, et al. 2021. Tectonics, climate and the diversification of the tropical African terrestrial flora and fauna. *Biological Reviews of the Cambridge Philosophical Society*, **96**(1): 16–51.

Cuypers LN, Sabuni C, Šumbera R, et al. 2022. Biogeographical importance of the livingstone mountains in southern Tanzania: comparative genetic structure of small non-volant mammals. *Frontiers in Ecology and Evolution*, **9**: 742851.

De Queiroz A, Gatesy J. 2007. The supermatrix approach to systematics. *Trends in Ecology & Evolution*, **22**(1): 34–41.

deMenocal P, Ortiz J, Guilderson T, et al. 2000. Abrupt onset and termination of the African Humid Period: rapid climate responses to gradual insolation forcing. *Quaternary Science Reviews*, **19**(1-5): 347–361.

deMenocal PB. 2004. African climate change and faunal evolution during the Pliocene–Pleistocene. *Earth and Planetary Science Letters*, **220**(1-2): 3–24.

Denys C, Lalis A, Aniskin V, et al. 2020. Integrative taxonomy of Guinean *Lemniscomys* species (Rodentia, Mammalia). *Journal of Vertebrate Biology*, **69**(2): 20008.

Denys C, Lecompte E, Dubois A, et al. 2017. Diagnoses and content of new African and Eurasian Murinae (Rodentia, Muridae) tribes. *Dumerilia*, **7**: 82–90.

Dobigny G, Tatard C, Gauthier P, et al. 2013. Mitochondrial and nuclear genes-based phylogeography of *Arvicanthis niloticus* (Murinae) and sub-Saharan open habitats pleistocene history. *PLoS One*, **8**(11): e77815.

Dolan AM, Haywood AM, Hunter SJ, et al. 2015. Modelling the enigmatic Late Pliocene glacial event — marine isotope stage M2. *Global and Planetary Change*, **128**: 47–60.

Dommain R, Riedl S, Olaka LA, et al. 2022. Holocene bidirectional river system along the Kenya Rift and its influence on East African faunal exchange and diversity gradients. *Proceedings of the National Academy of Sciences of the United States of America*, **119**(28): e2121388119.

Douglas J, Jiménez-Silva CL, Bouckaert R. 2022. StarBeast3: adaptive parallelized bayesian inference under the multispecies coalescent. *Systematic Biology*, **71**(4): 901–916.

Ducroz JF, Volobouev V, Granjon L. 2001. An assessment of the systematics of arvicanthine rodents using mitochondrial DNA sequences: evolutionary and biogeographical implications. *Journal of Mammalian Evolution*, **8**(3): 173–206.

Elith J, Leathwick JR. 2009. Species distribution models: ecological explanation and prediction across space and time. *Annual Review of Ecology, Evolution, and Systematics*, **40**: 677–697.

Farias IP, Ortí G, Sampaio I, et al. 2001. The cytochrome *b* gene as a phylogenetic marker: the limits of resolution for analyzing relationships among cichlid fishes. *Journal of Molecular Evolution*, **53**(2): 89–103.

Fordham DA, Saltré F, Haythorne S, et al. 2017. PaleoView: a tool for generating continuous climate projections spanning the last 21 000 years at regional and global scales. *Ecography*, **40**(11): 1348–1358.

Franklin J, Serra-Diaz JM, Syphard AD, et al. 2016. Global change and terrestrial plant community dynamics. *Proceedings of the National Academy of Sciences of the United States of America*, **113**(14): 3725–3734.

Friant S, Mistrick J, Luis AD, et al. 2025. Reducing the threats of rodent-borne zoonoses requires an understanding and leveraging of three key pillars: disease ecology, synanthropy, and rodentation. *The Lancet Planetary Health*, 101300.

Frost P. 1996. The ecology of miombo woodlands. *In*: Campbell B. The Miombo in Transition: Woodlands and Welfare in Africa. Bogor: Center for International Forestry Research, 11–58.

Fujisawa T, Barraclough TG. 2013. Delimiting species using single-locus data and the Generalized Mixed Yule Coalescent approach: a revised method and evaluation on simulated data sets. *Systematic Biology*, **62**(5): 707–724.

Fujita MK, Leaché AD, Burbrink FT, et al. 2012. Coalescent-based species delimitation in an integrative taxonomy. *Trends in Ecology & Evolution*, **27**(9): 480–488.

García-Peña GE, Rubio AV, Mendoza H, et al. 2021. Land-use change and rodent-borne diseases: hazards on the shared socioeconomic pathways. *Philosophical Transactions of the Royal Society B: Biological Sciences*, **376**(1837): 20200362.

Gibernau M, Montuire S. 1996. Mammal diversity and environment evolution during the Plio-Pleistocene in East Africa. *Human Evolution*, **11**(3): 193–204.

Guillory WX, Brown JL. 2021. A new method for integrating ecological niche modeling with phylogenetics to estimate ancestral distributions. *Systematic Biology*, **70**(5): 1033–1045.

Halliday JEB, Knobel DL, Agwanda B, et al. 2015. Prevalence and diversity of small mammal-associated *Bartonella* species in rural and urban Kenya. *PLoS Neglected Tropical Diseases*, **9**(3): e0003608.

Hammer Ø, Harper DAT. 2024. Paleontological Data Analysis. 2nd ed. Hoboken: John Wiley & Sons Ltd. doi: 10.1002/9781119933960.

Han BA, Kramer AM, Drake JM. 2016. Global patterns of zoonotic disease in mammals. *Trends in Parasitology*, **32**(7): 565–577.

Han BA, O'Regan SM, Schmidt JP, et al. 2020. Integrating data mining and transmission theory in the ecology of infectious diseases. *Ecology Letters*, **23**(8): 1178–1188.

Handika H, Esselstyn JA. 2024. SEGUL: ultrafast, memory-efficient and mobile-friendly software for manipulating and summarizing phylogenomic datasets. *Molecular Ecology Resources*, **24**(7): e13964.

Hánová A, Konečný A, Nicolas V, et al. 2021. Multilocus phylogeny of African striped grass mice (*Lemniscomys*): stripe pattern only partly reflects evolutionary relationships. *Molecular Phylogenetics and Evolution*, **155**: 107007.

Happold D. 2013. Lemniscomys striatus Striated Grass Mouse (Striated Lemniscomys). *In*: Happold D. Mammals of Africa Volume III: Rodents, Hares and Rabbits. London: Bloomsbury Publishing, 452–453.

Hernangómez D. 2023. Using the tidyverse with terra objects: the tidyterra package. *The Journal of Open Source Software*, **8**(91): 5751.

Hijmans RJR, Bivand R, Cordano E, et al. (2024-04-25). terra: Spatial Data

Analysis. R package version 1.7-83. https://cran.r-project.org/web/packages/terra/index.html.
Hill DJ. 2015. The non-analogue nature of Pliocene temperature gradients. *Earth and Planetary Science Letters*, **425**: 232–241.
Hu WQ, Li XY, Onditi KO, et al. 2025. Spatiotemporal distribution patterns of large and medium-sized mammals in a biodiversity hotspot: implications for conservation. *Biological Conservation*, **301**: 110863.
Huhndorf MH, Peterhans JCK, Loew SS. 2007. Comparative phylogeography of three endemic rodents from the Albertine Rift, east central Africa. *Molecular Ecology*, **16**(3): 663–674.
Huntley BJ. 2023. The afromontane forest and montane grassland biome. *In*: Huntley BJ. Ecology of Angola: Terrestrial Biomes and Ecoregions. Cham: Springer, 305–312.
Irwin DM, Kocher TD, Wilson AC. 1991. Evolution of the cytochrome *b* gene of mammals. *Journal of Molecular Evolution*, **32**(2): 128–144.
Kalyaanamoorthy S, Minh BQ, Wong TKF, et al. 2017. ModelFinder: fast model selection for accurate phylogenetic estimates. *Nature Methods*, **14**(6): 587–589.
Kapli P, Lutteropp S, Zhang J, et al. 2017. Multi-rate Poisson tree processes for single-locus species delimitation under maximum likelihood and Markov chain Monte Carlo. *Bioinformatics*, **33**(11): 1630–1638.
Katoh K, Standley DM. 2013. MAFFT multiple sequence alignment software version 7: improvements in performance and usability. *Molecular Biology and Evolution*, **30**(4): 772–780.
Kawakami M, Yamamura KI. 2008. Cranial bone morphometric study among mouse strains. *BMC Evolutionary Biology*, **8**(1): 73.
Klinges DH, Maclean IM, Scheffers BR. 2025. Redrawing Köppen-Geiger classes with microclimate: implications for nature and society. *Frontiers in Ecology and the Environment*, **23**(5): e2831.
Knoke T, Hanley N, Roman-Cuesta RM, et al. 2023. Trends in tropical forest loss and the social value of emission reductions. *Nature Sustainability*, **6**(11): 1373–1384.
Kokkinopoulou I, Moutsatsou P. 2021. Mitochondrial glucocorticoid receptors and their actions. *International Journal of Molecular Sciences*, **22**(11): 6054.
Korneliussen TS, Moltke I, Albrechtsen A, et al. 2013. Calculation of Tajima's *D* and other neutrality test statistics from low depth next-generation sequencing data. *BMC Bioinformatics*, **14**(1): 289.
Kottek M, Grieser J, Beck C, et al. 2006. World map of the Köppen-Geiger climate classification updated. *Meteorologische Zeitschrift*, **15**(3): 259–263.
Krásová J, Mikula O, Bryja J, et al. 2021. Biogeography of Angolan rodents: the first glimpse based on phylogenetic evidence. *Diversity and Distributions*, **27**(12): 2571–2583.
Kuhn JH, Adkins S, Alkhovsky SV, et al. 2025. Annual (2024) taxonomic update of RNA-directed RNA polymerase-encoding negative-sense RNA viruses (realm *Riboviria*: kingdom *Orthornavirae*: phylum *Negarnaviricota*). *Journal of General Virology*, **106**(6): 002077.
Kumar S, Stecher G, Suleski M, et al. 2024. MEGA12: molecular evolutionary genetic analysis version 12 for adaptive and green computing. *Molecular Biology and Evolution*, **41**(12): msae263.
Lahmam M, El M'rabet A, Ouarour A, et al. 2008. Daily behavioral rhythmicity and organization of the suprachiasmatic nuclei in the diurnal rodent. *Lemniscomys barbarus. Chronobiology International*, **25**(6): 882–904.
Lecompte E, Aplin K, Denys C, et al. 2008. Phylogeny and biogeography of African Murinae based on mitochondrial and nuclear gene sequences, with a new tribal classification of the subfamily. *BMC Evolutionary Biology*, **8**(1): 199.
Leigh JW, Bryant D. 2015. POPART: full-feature software for haplotype network construction. *Methods in Ecology and Evolution*, **6**(9): 1110–1116.
Leirs H, Kirkpatrick L, Sluydts V, et al. 2023. Twenty-nine years of continuous monthly capture-mark-recapture data of multimammate mice (*Mastomys natalensis*) in Morogoro, Tanzania. *Scientific Data*, **10**(1): 798.
Li XC, Yu L, Sohl T, et al. 2016. A cellular automata downscaling based 1 km global land use datasets (2010–2100). *Science Bulletin*, **61**(21): 1651–1661.
Linder HP, De Klerk HM, Born J, et al. 2012. The partitioning of Africa: statistically defined biogeographical regions in sub-Saharan Africa. *Journal of Biogeography*, **39**(7): 1189–1205.
Liu CR, White M, Newell G. 2013. Selecting thresholds for the prediction of species occurrence with presence-only data. *Journal of Biogeography*, **40**(4): 778–789.
Luo AR, Ling C, Ho SYW, et al. 2018. Comparison of methods for molecular species delimitation across a range of speciation scenarios. *Systematic Biology*, **67**(5): 830–846.
Mace GM, Collen B, Fuller RA, et al. 2010. Population and geographic range dynamics: implications for conservation planning. *Philosophical Transactions of the Royal Society B: Biological Sciences*, **365**(1558): 3743–3751.
Maley J, Doumenge C, Giresse P, et al. 2018. Late Holocene forest contraction and fragmentation in central Africa. *Quaternary Research*, **89**(1): 43–59.
Malhi Y, Adu-Bredu S, Asare RA, et al. 2013. African rainforests: past, present and future. *Philosophical Transactions of the Royal Society B: Biological Sciences*, **368**(1625): 20120312.
Mangombi JB, N'dilimabaka N, Lekana-Douki JB, et al. 2021. First investigation of pathogenic bacteria, protozoa and viruses in rodents and shrews in context of forest-savannah-urban areas interface in the city of Franceville (Gabon). *PLoS One*, **16**(3): e0248244.
Marchant R, Brewer S, Webb III T, et al. 2009. Holocene deforestation: a history of human–environmental interactions, climate change, and extinction. *In*: Turvey ST. Holocene Extinctions. Oxford: Oxford University Press, 213–234.
Matzke NJ. 2013a. Probabilistic historical biogeography: new models for founder-event speciation, imperfect detection, and fossils allow improved accuracy and model-testing. *Frontiers of Biogeography*, **5**(4): 242–248.
Matzke NJ. 2013b. BioGeoBEARS: BioGeography with Bayesian (and likelihood) evolutionary analysis in R Scripts. Berkeley: CRAN.
Matzke NJ. 2014. Model selection in historical biogeography reveals that founder-event speciation is a crucial process in island clades. *Systematic Biology*, **63**(6): 951–970.
Mawanda P, Rwego I, Kisakye JJ, et al. 2020. Rodents as potential hosts and reservoirs of parasites along the edge of a Central African forest: bwindi impenetrable national park, South Western Uganda. *African Health Sciences*, **20**(3): 1168–1178.
Mbou-Boutambe C, Boundenga L, Degrugillier F, et al. 2025. Rodent malaria parasites detected in the invasive *Rattus rattus* in Gabon. *International Journal for Parasitology: Parasites and Wildlife*, **27**: 101112.
Mikula O. 2018. Cutting tree branches to pick OTUs: a novel method of provisional species delimitation. *BioRxiv*, doi: https://doi.org/10.1101/419887.
Mikula O, Nicolas V, Šumbera R, et al. 2021. Nuclear phylogenomics, but not mitogenomics, resolves the most successful Late Miocene radiation of African mammals (Rodentia: Muridae: Arvicanthini). *Molecular Phylogenetics and Evolution*, **157**: 107069.
Minh BQ, Schmidt HA, Chernomor O, et al. 2020. IQ-TREE 2: new models and efficient methods for phylogenetic inference in the genomic era. *Molecular Biology and Evolution*, **37**(5): 1530–1534.
Missoup AD, Nicolas V, Eiseb S, et al. 2016. Phylogenetic position of the endemic Mount Oku rat, *Lamottemys okuensis* (Rodentia: Muridae), based on molecular and morphological data. *Zoological Journal of the Linnean Society*, **177**(1): 209–226.

Monadjem A, Taylor PJ, Denys C, et al. 2015. Rodents of Sub-Saharan Africa: a Biogeographic and Taxonomic Synthesis. Berlin: Walter de Gruyter GmbH & Co. KG.

Musila S, Chen ZZ, Li Q, et al. 2019. Diversity and distribution patterns of non-volant small mammals along different elevation gradients on Mt. Kenya, Kenya. *Zoological Research*, **40**(1): 53–60.

Mweu AW, Onditi KO, Khanal L, et al. 2024. Comparative phylogeography of two specialist rodents in forest fragments in Kenya. *Life*, **14**(11): 1469.

Neumann FH, Bamford MK. 2015. Shaping of modern southern African biomes: Neogene vegetation and climate changes. *Transactions of the Royal Society of South Africa*, **70**(3): 195–212.

Nicolas V, Mboumba JF, Verheyen E, et al. 2008. Phylogeographic structure and regional history of *Lemniscomys striatus* (Rodentia: Muridae) in tropical Africa. *Journal of Biogeography*, **35**(11): 2074–2089.

Ocón JP, Ibanez T, Franklin J, et al. 2021. Global tropical dry forest extent and cover: a comparative study of bioclimatic definitions using two climatic data sets. *PLoS One*, **16**(5): e0252063.

Olorunfemi IE, Olufayo AA, Fasinmirin JT, et al. 2022. Dynamics of land use land cover and its impact on carbon stocks in Sub-Saharan Africa: an overview. *Environment, Development and Sustainability*, **24**(1): 40–76.

Onditi KO, Demos TC, Peterhans JK, et al. 2021. Historical biogeography, systematics, and integrative taxonomy of the non-Ethiopian speckled pelage brush-furred rats (*Lophuromys flavopunctatus* group). *BMC Ecology and Evolution*, **21**(1): 89.

Onditi KO, Peterhans JK, Demos TC, et al. 2020. Morphological and genetic characterization of Mount Kenya brush-furred rats (*Lophuromys* Peters 1874); relevance to taxonomy and ecology. *Mammal Research*, **65**(2): 387–400.

Onditi KO, Song WY, Chen ZZ, et al. 2025. Multiscale spatial dependency of small mammal diversity patterns and their determinants. *Ecosphere*, **16**(2): e70179.

Onditi KO, Song WY, Li XY, et al. 2022. Patterns and predictors of small mammal phylogenetic and functional diversity in contrasting elevational gradients in Kenya. *Frontiers in Ecology and Evolution*, **9**: 742524.

Otto-Bliesner BL, Marshall SJ, Overpeck JT, et al. 2006. Simulating arctic climate warmth and icefield retreat in the last interglaciation. *Science*, **311**(5768): 1751–1753.

Ozeki T, Abe H, Ushijima Y, et al. 2022. Identification of novel orthonairoviruses from rodents and shrews in Gabon, Central Africa. *Journal of General Virology*, **103**(10): 001796.

Pennington PT, Cronk QCB, Richardson JA, et al. 2004. Mechanisms and tempo of evolution in the African Guineo–Congolian rainforest. *Philosophical Transactions of the Royal Society B: Biological Sciences*, **359**(1450): 1585–1594.

Phillips SJ, Anderson RP, Schapire RE. 2006. Maximum entropy modeling of species geographic distributions. *Ecological Modelling*, **190**(3-4): 231–259.

Pirani A, Fuglestvedt JS, Byers E, et al. 2024. Scenarios in IPCC assessments: lessons from AR6 and opportunities for AR7. *npj Climate Action*, **3**(1): 1.

Potts R, Faith JT. 2015. Alternating high and low climate variability: the context of natural selection and speciation in Plio-Pleistocene hominin evolution. *Journal of Human Evolution*, **87**: 5–20.

Puillandre N, Brouillet S, Achaz G. 2021. ASAP: assemble species by automatic partitioning. *Molecular Ecology Resources*, **21**(2): 609–620.

Puillandre N, Miralles A, Brouillet S, et al. 2024. Species delimitation and exploration of species partitions with ASAP and LIMES. *Methods in Molecular Biology*, **2744**: 313–334.

Rambaut A, Drummond AJ, Xie D, et al. 2018. Posterior summarization in bayesian phylogenetics using tracer 1.7. *Systematic Biology*, **67**(5): 901–904.

Ramírez-Soriano A, Ramos-Onsins SE, Rozas J, et al. 2008. Statistical power analysis of neutrality tests under demographic expansions, contractions and bottlenecks with recombination. *Genetics*, **179**(1): 555–567.

Rozas J. 2009. DNA sequence polymorphism analysis using DnaSP. *In*: Posada D. Bioinformatics for DNA Sequence Analysis. New York: Humana Press, 337–350.

Rozas J, Ferrer-Mata A, Sánchez-Delbarrio JC, et al. 2017. DnaSP 6: DNA sequence polymorphism analysis of large data sets. *Molecular Biology and Evolution*, **34**(12): 3299–3302.

Schradin C. 2008. Seasonal changes in testosterone and corticosterone levels in four social classes of a desert dwelling sociable rodent. *Hormones and Behavior*, **53**(4): 573–579.

Ségalen L, Lee-Thorp JA, Cerling T. 2007. Timing of C_4 grass expansion across sub-Saharan Africa. *Journal of Human Evolution*, **53**(5): 549–559.

Serneels S, Linderman M, Lambin EF. 2007. A multilevel analysis of the impact of land use on interannual land-cover change in East Africa. *Ecosystems*, **10**(3): 402–418.

Sikes RS, The Animal Care and Use Committee of the American Society of Mammalogists. 2016. 2016 Guidelines of the American Society of Mammalogists for the use of wild mammals in research and education. *Journal of Mammalogy*, **97**(3): 663–688.

Staps M, Miller PW, Tarnita CE, et al. 2023. Development shapes the evolutionary diversification of rodent stripe patterns. *Proceedings of the National Academy of Sciences of the United States of America*, **120**(45): e2312077120.

Starik N, Mbango OK, Bengsch S, et al. 2020. Landscape transformation influences responses of terrestrial small mammals to land use intensity in north-central Namibia. *Diversity*, **12**(12): 488.

Stork NE, Coddington JA, Colwell RK, et al. 2009. Vulnerability and resilience of tropical forest species to land-use change. *Conservation Biology*, **23**(6): 1438–1447.

The American Society of Mammalogist's Mammal Diversity Database. (2025-03-11). Mammal diversity database (version 2.0). Zenodo. https://doi.org/10.5281/zenodo.4139722.

The R Core Team. 2025. R: a language and environment for statistical computing. Vienna: R Foundation for Statistical Computing.

Tobe SS, Kitchener AC, Linacre AMT. 2010. Reconstructing mammalian phylogenies: a detailed comparison of the cytochrome *b* and cytochrome oxidase subunit I mitochondrial genes. *PLoS One*, **5**(11): e14156.

Trauth MH, Maslin MA, Deino A, et al. 2005. Late Cenozoic moisture history of East Africa. *Science*, **309**(5743): 2051–2053.

Trauth MH, Maslin MA, Deino AL, et al. 2007. High- and low-latitude forcing of Plio-Pleistocene East African climate and human evolution. *Journal of Human Evolution*, **53**(5): 475–486.

Underwood W, Anthony R. 2020. AVMA Guidelines for the Euthanasia of Animals: 2020 Edition. Schaumburg: American Veterinary Medical Association, 2020–2021.

Vences M, Miralles A, Brouillet S, et al. 2021. iTaxoTools 0.1: kickstarting a specimen-based software toolkit for taxonomists. *Megataxa*, **6**(2): 77–92.

Wickham H, Averick M, Bryan J, et al. 2019. Welcome to the tidyverse. *Journal of Open Source Software*, **4**(43): 1686.

Wilson DE, Lacher Jr TE, Mittermeier RA, et al. 2017. Handbook of the Mammals of the World, Volume 7: Rodents II. Barcelona: Lynx Edicions.

Wong TKF, Ly-Trong N, Ren H, et al. 2025. IQ-TREE 3: phylogenomic inference software using complex evolutionary models. https://doi.org/10.32942/X2P62N.

Xie JM, Chen YR, Cai GJ, et al. 2023. Tree Visualization By One Table (tvBOT): a web application for visualizing, modifying and annotating phylogenetic trees. *Nucleic Acids Research*, **51**(W1): W587–W592.